THE ASTROPHYSICAL JOURNAL, 414:846–866, 1993 September 10

X-RAY EMISSION AT THE LOW-MASS END: RESULTS FROM AN EXTENSIVE *EINSTEIN OBSERVATORY* SURVEY

M. BARBERA, G. MICELA, AND S. SCIORTINO
Istituto e Osservatorio Astronomico di Palermo, Palazzo dei Normanni, 90134 Palermo, Italy
F. R. HARNDEN, JR.
Harvard-Smithsonian Center for Astrophysics, 60 Garden Street, Cambridge, MA 02138
AND
R. ROSNER
Department of Astronomy and Enrico Fermi Institute, University of Chicago, 5640 South Ellis Avenue, Chicago, IL 60637
Received 1992 December 2; accepted 1993 March 3

ABSTRACT

We have used all the available data from the *Einstein Observatory* Imaging Proportional Counter (IPC), and a critical compilation of cataloged optical data, to measure the 0.16–3.5 keV X-ray emission from 88 K and 169 M stars of luminosity classes IV, V, and VI within 25 pc from the Sun. The IPC detected 54 out of the 88 K stars, 70 out of the 138 M stars with M_v less than 13.4 (corresponding approximately to M5), and 15 out of the 31 fainter M stars. We have identified a subsample of surveyed stars that is statistically representative of the population of K and M stars in the solar neighborhood. On the basis of this subsample (1) we have shown the occurrence of a drop in the level of X-ray emission for M stars later than approximately M5; (2) we have built *unbiased* maximum likelihood X-ray luminosity functions for the K, early M, and late M stars; (3) we have confirmed, both for K and M stars, the decrease of X-ray luminosity with increasing stellar age in the range of ages of disk population stars: and (4) we have shown that no obvious correlation is present between X-ray and bolometric luminosities in the entire representative samples of K and M stars, but only within flare stars which also seem to mark a saturation in X-ray luminosity level.

Subject headings: stars: late-type — X-ray: stars

1. INTRODUCTION

Since the first analysis of the X-ray data of the *Einstein* satellite (Giacconi et al. 1979) which has shown the pervasiveness of the X-ray emission throughout the H-R diagram (Vaiana et al. 1981), many stellar X-ray surveys have been carried out to characterize on a statistical basis the X-ray emission of normal stars selected according to spectral type and stellar age. Among these surveys we mention the following: late *d*A and *d*F stars (Schmitt et al. 1985), *d*G stars (Maggio et al. 1987), O stars (Sciortino et al. 1990), F-M giants (Maggio et al. 1990), B stars (Grillo et al. 1992), the Hyades (Stern et al. 1981; Micela et al. 1988), the Pleiades (Caillault & Helfand 1985; Micela et al. 1985, 1990), the Chamaleon region (Feigelson & Kriss 1989), and the Ursa Major stream (Walter et al. 1984; Schmitt et al. 1990a). In this paper we concentrate on the study of the X-ray emission of stars at the low-mass end, that is, K and M dwarf stars.

K and M stars are the most numerous in the solar neighborhood and throughout the whole Galaxy, and, because of their high X-ray emission level (as also shown below), they have been recognized as the most important stellar contributors to the soft X-ray background (see Rosner et al. 1981; Caillault et al. 1986; Schmitt & Snowden 1990; Kashyap et al. 1992). One of the crucial points in the exact evaluation of the expected stellar contribution to the X-ray background is the availability of an X-ray luminosity function of K and M stars derived from an unbiased, statistically representative sample. To find these X-ray luminosity functions is one of the aims of this work.

A further aim of this paper is to investigate the dependence of X-ray luminosity on spectral type at the low-mass end of the MS. In fact, previous work (Golub 1983; Bookbinder 1985; Rosner, Golub, & Vaiana 1985) based on the analysis of somewhat smaller size samples, has presented indications of a steep drop in X-ray emission occurring for stars later than M5, where stellar structure models predict that stars become fully convective. This observational fact, if confirmed by the analysis of a large statistically representative sample, could strengthen our comprehension of the mechanisms underlying the amplification of stellar magnetic fields which are responsible for the confinement of the hot coronal plasma. In order to test the occurrence of a drop in X-ray emission level at $\sim$M5, great attention must be paid to the possible biases present in the M star sample. For instance, high spatial incompleteness suffered at faint visual magnitudes in volume-limited optical samples needs to be investigated.

The availability of a large sample makes it possible to study the dependence of X-ray emission on physical parameters such as rotation and/or age. Since Pallavicini et al. (1981) have shown that the X-ray luminosity correlates with $v \sin i$ for stars later than F7 and suggested the relation $L_X = 10^{27} \times (v \sin i)^2$ ergs s^{-1} as the best fit to data, various authors have addressed the same problem on different samples, either optically selected (Mangenay & Praderie 1984; Marilli & Catalano 1984; Micela, Sciortino, & Serio 1984; Maggio et al. 1987; Schmitt et al. 1985) or X-ray selected (Fleming, Gioia, & Maccacaro 1989). All these works find a correlation between L_X and either $v \sin i$ or R_0 (the so-called Rossby number), even if with different functional relations. The observed relation between L_X and the rotation rate for the fast rotating K stars of the Pleiades seems to flatten with respect to the Pallavicini's relation (Caillault & Helfand 1985; Micela et al. 1985, 1990).

Unfortunately, rotation rates of nearby M dwarfs have been measured only for few objects, because of their intrinsic faintness and slow rotation rate, less than 10 km s^{-1} (Stauffer & Hartmann 1986; Marcy & Chen 1991). Hence, to establish the existence and the nature of the correlation between L_X and rotation rate for the late M stars is a very difficult, yet unresolved, task. Furthermore, studies conducted on open clusters and stellar associations such as the Pleiades (Caillault & Helfand 1985; Micela et al. 1985, 1990), the Hyades (Stern et al. 1981; Micela et al. 1988), the Ursa Major stream (Schmitt et al. 1990a), the Chamaleon region (Feigelson & Kriss 1989), and the Taurus-Auriga (Damiani & Micela 1993) have established the decrease of X-ray emission level with increasing age. Since K and M stars evolve on a time scale greater than 10^{10} yr, they have not yet left the main sequence and represent all the epochs of stellar formation in the Galaxy. This simple fact makes low-mass stars fundamental for the study of age-related properties of the Galaxy, such as star formation rate and/or kinematical evolution.

In this framework, this work is aimed to a detailed statistical analysis of the X-ray emission of low-mass stars (spectral types K and M and luminosity classes IV, V, and VI) in the solar neighborhood. We endeavor to accomplish such a task by (1) using a wider and better-known optical volume-limited sample, (2) accurately investigating the possible occurrence of sample selection effects, and (3) using all the available *Einstein* IPC data reduced homogeneously with the latest processing (REV-1, Harnden et al. 1984). Previous surveys of K and M stars had been based on preliminary versions of the *Einstein* IPC data processing.

Our paper is organized as follows: § 2 describes the stellar sample used in this work; § 3 presents the X-ray data and methodologies used to estimate the stellar X-ray luminosity; in § 4 we present the main results which are discussed in further detail in § 5; and a summary of the work is given in § 6.

2. SAMPLE SELECTION

2.1. *The Optical Sample*

To minimize the incompleteness suffered at faint magnitudes by volume-limited samples, we have merged data from the three optical catalogs below.

1. The *Near Star Catalogue* (Gliese 1969) which includes data available until 1968 (1899 stars) for the known stars within 22 pc from the Sun. For 377 of these stars, the measure of the parallax has been updated using new data published in 1979 (Gliese & Jahreiss 1979).
2. A supplement to the *Near Star Catalogue* (Gliese & Jahreiss 1979) listing 333 stars within 22 pc from the Sun.
3. The *Catalogue of Stars within 25 Parsecs from the Sun* (Woolley, Penstom, & Pocock 1970) including 2150 stars.

The optical sample we have obtained through this compilation contains about 30% more stars than those we would have selected using only the Woolley catalog. This enlarged number does not, however, guarantee the completeness of the optical sample.

We have selected from the above optical catalogs: (1) stars with spectral types K or M and luminosity classes IV, V, VI; (2) stars located on the main sequence in the proper range of absolute visual magnitude ($5 \leq M_v < 8.5$ for the K stars and $M_v \geq 8.5$ for the M stars), and color index $B-V$ or $R-I$ ($0.76 < B-V < 1.42$ or $0.2 < R-I < 0.7$ for the K stars and $1.3 < B-V < 2.3$ or $0.6 < R-I < 2.5$ for the M stars); (3) stars with spectral types K or M, unknown luminosity class, and absolute visual magnitude in the range of interest; and (4) those stars lacking any information about spectral type, luminosity class, and color index but with absolute visual magnitude in the range of interest. Our integrated optical sample contains 1035 M stars[1] (618 of groups 1 and 2, 260 of group 3, and 157 of group 4) and 633 K stars (508 of groups 1 and 2, 56 of group 3, and 69 of group 4). We have estimated that the fourth group of M stars may be contaminated by ~ 16 white dwarfs.[2]

In order to characterize our sample in terms of age, we have homogeneously recomputed the U, V, W components of stellar velocity with respect to the Sun from the available data of proper motion, radial velocity, and parallax following the method described by Johnson & Soderblom (1987), choosing a righthanded frame of reference with positive axes pointing, respectively, toward the center of Galaxy, along the tangential rotational velocity of Galaxy, and toward the North Galactic Pole.

We have subdivided the stars of the optical sample with known U, V, W velocity components in young disk, old disk, and halo population stars (see row 1 in Table 2 and Fig. 1) according to a statistical method based on the U and V velocity components (Eggen 1973a, 1973b, 1973c). The irregular polygon reported in Figure 1 delimits the region of kinematically young disk stars, the region between the polygon and the ellipse is populated by kinematically old disk stars, while the region outside the ellipse is populated by halo population stars. This method of age classification is calibrated on the U and V velocity distribution of stars whose age is known according to an assumed evolutionary model. The region of the U-V plane pertaining to the very young disk population (between 2 and 7×10^7 yr) has been defined by studying a sample of very bright B-type field stars and some B-type members of the Pleiades group (Eggen 1973a). The region of the young disk population (up to the age of the Hyades, i.e., between 5 and 8×10^8 yr) has been derived from a sample of main-sequence and near-main-sequence A-type stars (Eggen 1973b). Finally, the region of the old disk population has been derived from a sample of F and early G-type stars brighter than visual magnitude 6.5 (Eggen 1973c). As it is evident, this method is based only on observational evidence and does not require the assumption of any model of stellar kinematical evolution. Other statistical methods have been presented in the literature to separate stars in different age groups according to their kinematical properties; in § 4 we shall briefly discuss two of these and compare them with the one we have adopted.

To evaluate the spatial completeness of our optical parent sample we have adopted a method originally developed for quasars (Schmidt 1968) and later extended to study the stellar galaxy distribution (Upgren & Armandroff 1981).

Consider a subsample of stars within a range of absolute visual magnitudes. Given a sphere of volume V_{max} (smaller than the sphere of 25 pc radius limiting our catalog), we compute the average $\langle V/V_{max} \rangle$ where V is the volume enclosed by each star of the subsample (i.e., $\frac{4}{3}\pi R^3$ where R is the star's distance from the Sun). If the considered subsample consists of N stars

[1] For the sake of uniformity, in the paper we consider M stars those with absolute visual magnitude ≥ 8.5.

[2] This estimate is based on the fraction between the number of white dwarfs and the number of M stars within 25 pc from the Sun, in the same range of absolute visual magnitude, as obtained from the Woolley catalog.

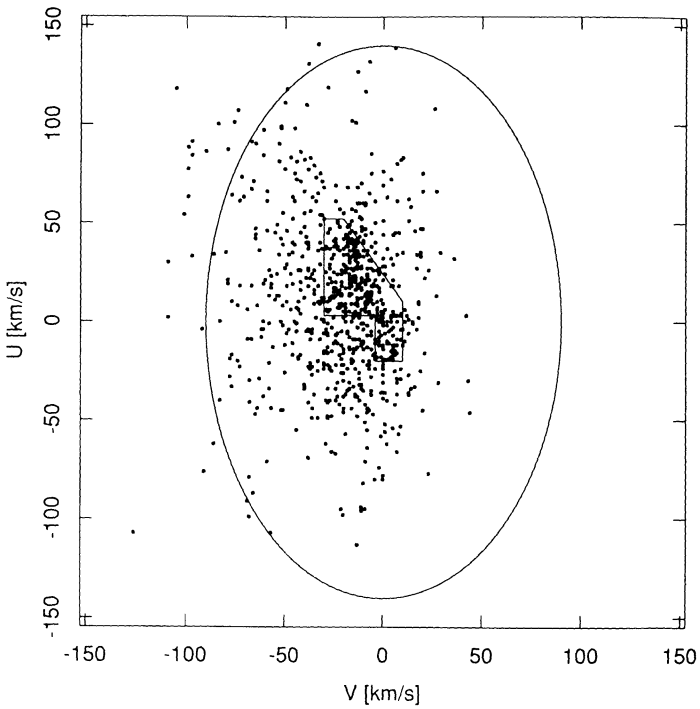

FIG. 1.—Scatter plot of U vs. V space velocity components for the stars of the optical sample. According to the criterion by Eggen (1973a, 1973b, 1973c) the irregular polygon delimits the region populated by kinematically young stars, and the ellipse separates the region populated by kinematically old stars (inside) from the region populated by halo population stars.

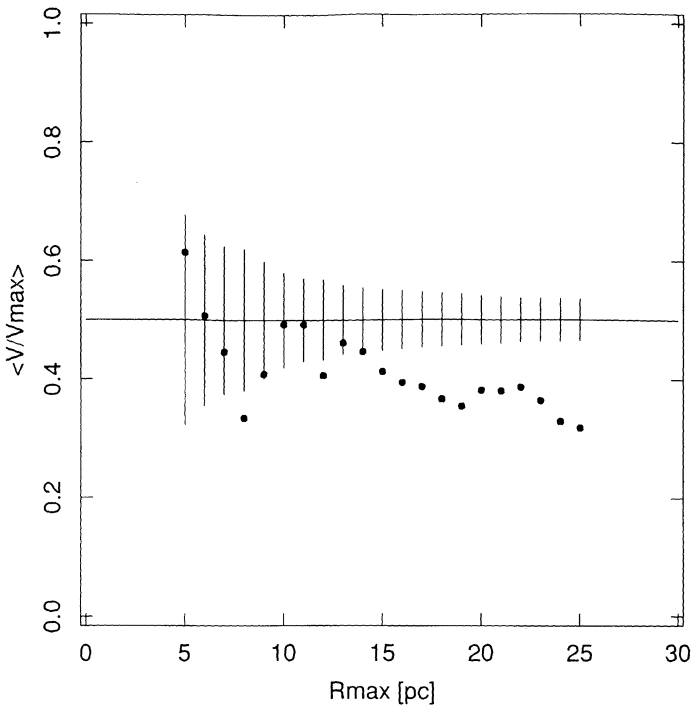

FIG. 2.—$\langle V/V_{max}\rangle$ as a function of R_{max} (the radius corresponding to a sphere of volume V_{max}) for the subsample of stars with $11.5 < M_v \leq 12.5$ (*solid dots*). The expectation vaiue 0.5 and 3 σ uncertainties in the hypothesis of stars randomly distributed within V_{max} are also plotted.

randomly distributed within V_{max}, the quantity $\langle V/V_{max}\rangle$ is Poisson-distributed with expectation value $E = 0.5$ and variance $\sigma^2 = 1/12N$ (Avni & Bahcall 1980). Computing $\langle V/V_{max}\rangle$ for different values of V_{max}, it is possible to find a range of volumes within which our subsample of stars may be considered uniformly distributed. As an example we show in Figure 2 $\langle V/V_{max}\rangle$ as a function of R_{max} (the radius corresponding to the sphere of volume V_{max}) for the subsample of stars with $11.5 < M_v \leq 12.5$, together with the expectation value 0.5 and the 3 σ statistical uncertainties (we have considered in the analysis only integral values of R_{max} between 5 and 25 pc). The results indicate that the stars in this subsample can be considered uniformly distributed in the range of radii from 5 up to 13 pc.

Once this range of R_{max} has been determined, a stellar density can be evaluated within each corresponding sphere of volume $V_{max}\{\rho(R_{max}) = N(R_{max})/[(4/3)\pi R^3_{max}]\}$, along with a statistical error $\{\Delta\rho(R_{max}) = [N(R_{max})]^{1/2}/[(4/3)\pi R^3_{max}]\}$, where $N(R)$ is the number of stars within R. The expected density of stars in the solar neighborhood is then evaluated as the weighted mean $\Sigma[\rho(R_{max})/\Delta\rho(R_{max})^2]/\Sigma[1/\Delta\rho(R_{max})^2]$, and its uncertainty is defined by the maximum and minimum values of $\rho(R_{max})$ in the above range of R_{max}. The density obtained in this way allows an estimate of the number of stars within the 25 pc sphere limiting our survey.

We have carried out this procedure for various subsamples of stars selected according to the absolute visual magnitude ($4.5 < M_v \leq 5.5$, $5.5 < M_v \leq 6.5$, ...), and we have evaluated the expected number of stars per unit magnitude within 25 pc from the Sun as a function of M_v. We have compared this expectation with the optical luminosity function determined by Wielen, Jahreiss, & Kruger (1983, hereafter WJK) for the low-mass stars in the solar neighborhood, and we have found our determination in agreement, within error bars, except in the range of absolute visual magnitude $13.5 \leq M_v \leq 17.5$, where the WJK luminosity function is dominated by the white dwarfs, which are not included in our sample.

In Figure 3 we have compared the expected number of stars inside 25 pc from the Sun (asterisks and dashed line bars) to the number of stars present in our catalog (solid histogram) as a function of M_v. We can see that our catalog may be considered complete within 25 pc for $M_v \leq 9$, while it is incomplete by a factor 3 in the range $9 < M_v < 13$. For $M_v > 13$ our sample is even 10 times less numerous than the expected one. As was expected, the optical parent sample of M stars is not uniformly sampled in M_v. This evidence must be properly considered when building X-ray luminosity functions of stars in a large range of spectral types.

2.2. *The X-Ray Sample*

The X-ray sample is composed of stars of the optical sample which fall, either serendipitously or as targets, in at least one of the fields of the *Einstein* IPC. It consists of the 257 stars listed in Table 1. In the same way as we have done for the optical sample, we have estimated that there may be about two white dwarfs among the 22 stars of unknown spectral type and luminosity class, and therefore we are confident that this possible contamination will not alter any of our results. Table 1 lists also the U, V stellar velocity components we have used to subdivide the stars of the X-ray sample in young disk, old disk, and halo population stars, according to Eggen's criteria previously described.

TABLE 1

SURVEYED K AND M STARS

GLIESE number (1)		RA(1950) h m s (2)			DEC(1950) d m s (3)			m_v (4)	B - V (5)	M_v (6)	Sp (7)	Dist. (pc.) (8)	U	V	W (9)	Age Flag (10)	Rate $cts\ s^{-1}$ (11)	Error $cts\ s^{-1}$ (12)	$\log(L_x)$ $erg\ s^{-1}$ (13)	Rate Flag (14)	Point. Flag (15)	Notes (16)
5.0		0	4	1	28	44	42	6.14	0.75	5.33	K0	14.5	15	-23	-10	Y	0.188	0.017	29.13	M	S	
15.0	A	0	15	31	43	44	24	8.08	1.56	10.39	M1	3.4	47	-10	-3	O	0.021	0.006	26.62	M	P	
15.0	B	0	15	31	43	44	24	11.06	1.80	13.37	M6	3.4	50	-4	-6	O	0.021	0.006	26.62	M	P	
27.0		0	36	45	20	58	54	5.86	0.85	5.77	K0	10.4	-38	-20	10	O	< 0.009		< 27.50	L	P	
33.0		0	45	45	5	1	24	5.76	0.88	6.54	K2	7.0	0	-45	-10	O	< 0.009		< 27.17	L	P	
34.0	B	0	46	3	57	33	6	7.51	1.39	8.68	M0	5.8	31	-6	-15	Y	0.018	0.004	27.02	M	P	
38.0		0	48	23	58	1	30	10.67		9.37	M2 V	18.2	100	-84	40	H	< 0.043		< 28.68	L	S	
56.3	A	1	16	6	-1	7	36	8.00	0.82	6.31	K1	21.7	26	-42	-18	O	0.004	0.001	27.46	M	S	
56.3	B	1	16	5	-1	7	60	10.73	1.40	9.04	M0	21.7	26	-42	-18	O	0.004	0.001	27.46	M	S	
65.0	A	1	36	25	-18	12	42	12.52		15.46	M5.5 V	2.6	42	-18	-19	Y	0.204	0.004	27.37	ML	P	v
65.0	B	1	36	25	-18	12	42	13.02		15.96	M5.5 V	2.6	43	-18	-22	Y	0.204	0.004	27.37	ML	P	v
66.0	A	1	37	54	-56	26	54	5.74	0.88	6.59	K2	6.8	3	-14	-16	Y	0.021	0.004	27.21	M	S	
66.0	B	1	37	54	-56	26	53	5.90		6.82	K0 V	6.5	3	-14	-15	Y	0.021	0.004	27.18	M	S	
70.0		1	40	46	4	4	54	10.95	1.59	11.24	M2 V	8.8	-29	-12	-17	O	< 0.010		< 27.43	L	S	
83.1		1	57	28	12	50	6	12.27	1.80	14.02	M8 V	4.5					0.060	0.005	27.61	M	P	
85.1		2	7	7	35	12	0	15.00		13.31	M3	21.7					< 0.007		< 28.03	L	S	
86.0		2	8	25	-51	4	6	6.11	0.82	5.86	K0	11.2	101	-76	-25	H	0.012	0.004	27.72	M	S	
97.2		2	22	52	59	26	6	6.92		5.92	K0	15.9	18	8	0	O	< 0.006		< 27.70	L	S	
103.0		2	32	28	-43	59	24	8.70	1.39	8.42	K7	11.4	-6	-30	-32	O	0.629	0.042	29.44	L	P	
105.0	A	2	33	20	6	39	0	5.82	0.97	6.50	K3	7.3	76	0	34	O	0.006	0.001	27.05	M	P	
105.0	B	2	33	31	6	37	60	11.65	1.61	12.33	M4 V	7.3	76	0	34	O	< 0.004		< 26.83	L	P	
117.0		2	50	7	-12	58	18	6.05	0.87	6.57	K0	7.9	14	-16	-11	Y	0.187	0.010	28.60	M	P	
142.0		3	25	36	-19	58	54	8.37	1.34	7.63	K7	14.1	49	-17	-3	O	0.022	0.003	28.17	M	P	
144.0		3	30	34	-9	37	36	3.73	0.88	6.14	K2	3.3	3	7	-20	Y	0.435	0.032	28.21	L	P	
157.0	A	3	54	57	-1	18	0	8.06	1.12	8.10	K5 V	9.8	-2	0	-12	Y	0.062	0.010	28.01	M	P	
157.0	B	3	54	57	-1	18	0	11.48	1.52	11.52	M3 V	9.8	3	-1	-17	Y	0.062	0.010	28.01	M	P	
166.0	A	4	12	58	-7	43	48	4.43	0.82	6.01	K1	4.8	-94	-11	-39	O	0.164	0.008	27.58	M	P	h
166.0	C	4	13	4	-7	44	6	11.17	1.68	12.75	M4.5 V	4.8	-96	-11	-36	O	0.164	0.008	28.00	M	P	h
168.1		4	19	15	19	21	54	16.00		15.19		14.5					< 0.006		< 27.63	L	S	
168.2		4	19	18	19	22	6	17.30		16.12		17.2					< 0.005		< 27.74	L	S	
171.1	B	4	33	3	16	24	36	13.50		12.00	M2 V	20.0	48	-18	-24	Y	< 0.009		< 28.11	L	P	
171.2	A	4	33	42	27	1	60	8.42	1.12	7.35	K5 V	16.4	39	-15	0	Y	0.563	0.022	29.71	ML	P	
172.0		4	33	43	52	47	60	8.61	1.41	8.45	K8	10.8	44	-9	-1	O	0.006	0.002	27.40	M	S	
180.0		4	51	35	-17	50	42	12.50		12.10	M3	12.0					< 0.009		< 27.63	L	S	
182.0		4	56	59	1	42	36	10.05		8.41	M1 V	21.3	26	-19	-26	Y	0.256	0.009	29.60	ML	P	v
183.0		4	58	20	-5	48	36	6.21	1.06	6.40	K3	9.2	-1	-58	-13	O	0.007	0.002	27.31	M	P	
191.0		5	9	41	-44	59	54	8.81	1.56	10.85	M0	3.9	-19	-288	-52	H	< 0.010		< 26.70	L	P	
195.0	A	5	13	42	45	47	30	10.20	1.50	9.60	M2 V	13.2	41	-10	-8	O	< 0.018		< 28.04	L	P	
195.0	B	5	13	42	45	47	30	13.70		13.10	M5 V	13.2	41	-10	-8	O	< 0.018		< 28.04	L	P	
201.0		5	20	43	17	16	42	7.97	1.09	6.97	K5 V	15.9	37	-15	9	Y	0.012	0.004	28.02	M	P	
206.0		5	29	30	9	47	18	11.50	1.62	10.73	M4 V	14.3	10	-7	-22	Y	0.152	0.008	29.03	L	P	
207.1		5	31	9	1	54	48	11.68		10.78	M3 V	15.2					0.147	0.008	29.06	M	P	
213.0		5	39	14	12	29	18	11.48	1.65	12.58	M5.5 V	6.0	86	-90	9	H	0.015	0.004	27.27	M	P	
217.2		5	45	6	-70	10	48	8.09	0.76	6.45	K0	21.3	117	-9	-47	O	< 0.008		< 28.11	L	S	
229.0		6	8	28	-21	50	36	8.13	1.50	9.32	M1	5.8	-12	-11	-11	O	0.009	0.001	26.99	M	P	

TABLE 1—*Continued*

GLIESE number (1)		RA(1950) h	m	s (2)	DEC(1950) d	m	s (3)	m_v (4)	B - V (5)	M_v (6)	Sp (7)	Dist. (pc.) (8)	U	V	W ($Km \cdot s^{-1}$) (9)	Age Flag (10)	Rate $cts\ s^{-1}$ (11)	Error $cts\ s^{-1}$ (12)	$\log(L_x)$ $erg\ s^{-1}$ (13)	Rate Flag (14)	Point. Flag (15)	Notes (16)
233.0		6	23	14	18	47	18	6.76	0.94	5.79	K3 V	15.6	-16	-4	-14	Y	0.287	0.015	29.08	M	P	
233.0	B	6	23	14	18	47	17	13.80		13.40		12.0					0.287	0.015	28.85	M	P	
234.0	A	6	26	51	-2	46	12	11.15	1.74	13.11	M7 V	4.1	10	-28	3	Y	0.096	0.006	27.43	M	P	
234.0	B	6	26	51	-2	46	12	14.50		16.46		4.1	10	-28	3	Y	0.096	0.006	27.43	M	P	
241.0		6	38	12	24	0	36	8.14	1.02	7.49	K6 V	13.5	-48	-13	-2	O	0.006	0.002	27.54	M	P	
250.0	A	6	49	52	-5	6	42	6.60	1.05	6.69	K6 V	9.6	-1	15	-21	O	0.031	0.005	27.68	M	P	
250.0	B	6	49	52	-5	7	42	10.11	1.50	10.20	M2	9.6	-1	15	-21	O	0.031	0.005	27.68	M	P	
263.0		7	1	56	-10	25	18	11.30		10.19	M5	16.7					< 0.005		< 27.68	L	S	
268.0		7	6	39	38	37	30	11.48	1.71	12.58	M5 V	6.0	44	-19	-8	Y	0.041	0.004	27.70	M	P	
273.0		7	24	43	5	22	42	9.82	1.56	11.94	M5 V	3.8	-9	-69	-15	O	< 0.007		< 26.55	L	P	
278.0	C	7	31	26	31	58	48	9.07	1.49	8.26	M0.5	14.5	7	-3	-13	Y	0.468	0.026	29.53	ML	P	
283.0	B	7	38	2	-17	17	24	17.60		18.36	M	7.0					< 0.004		< 26.82	L	P	
285.0		7	42	4	3	40	48	11.20	1.59	12.31	M4.5 V	6.0	13	-17	-11	Y	0.377	0.008	28.66	ML	P	v,h
295.1		7	57	28	13	56	12	10.30	1.28	9.04	K5 V	17.9	25	-19	1	Y	< 0.012		< 28.10	L	S	
319.1	A	8	40	22	-42	44	54	8.10	0.90	6.55	K0	20.4					< 0.044		< 28.80	L	S	
319.1	B	8	40	22	-42	45	36	14.30		12.75	M1	20.4					< 0.044		< 28.80	L	S	
321.3	B	8	43	19	-54	31	30	5.10		3.51		20.8	-7	-1	-3	Y	0.048	0.005	28.38	M	P	
321.3	C	8	43	26	-54	30	54	11.00		9.41		20.8	-7	-1	-3	Y	0.048	0.005	28.38	M	P	
321.3	D	8	43	26	-54	30	54	13.50		11.91		20.8	-7	-1	-3	Y	0.048	0.005	28.38	M	P	
323.0	A	8	48	2	8	3	6	9.78	1.34	8.56	M0 V	17.5	-3	5	-8	Y	0.031	0.005	28.21	M	S	
323.0	B	8	48	2	8	3	6	9.90		8.83		16.4	-3	5	-8	Y	0.031	0.005	28.15	M	S	
324.0	B	8	49	42	28	30	30	13.15	1.65	12.50	M5	13.5	38	-19	-10	Y	0.003	0.001	26.94	M	P	
331.0	B	8	55	48	48	14	24	10.80		9.90	M1 V	15.2	33	-13	-13	Y	0.038	0.006	28.17	M	P	
331.0	C	8	55	48	48	14	24	11.10		10.20		15.2	31	-14	-15	Y	0.038	0.006	28.17	M	P	
334.0		9	4	20	-8	36	30	9.50	1.42	9.12	M0 V	11.9	33	-16	7	Y	0.009	0.003	27.62	M	P	
340.2		9	16	54	1	6	36	7.90		6.31	K0	20.8	26	-35	7	O	< 0.008		< 28.07	L	S	
343.1		9	24	20	39	43	30	9.88	1.32	8.10	K8 V	22.7	-26	-12	-4	O	0.023	0.003	28.61	M	S	
346.0		9	26	24	-9	2	48	10.49	1.41	9.15	M0 V	18.5					< 0.037		< 28.64	L	S	
349.0		9	27	19	5	52	24	7.21	1.00	6.93	K3	11.4	36	-13	0	Y	0.027	0.004	28.07	M	P	
363.0		9	38	57	56	13	12	14.20		13.46	M5	14.1					< 0.009		< 27.81	L	S	
380.0		10	8	19	49	42	30	6.59	1.36	8.32	K7	4.5	7	-19	-34	Y	0.077	0.005	27.73	M	P	
384.0	B	10	10	56	-47	13	48	10.80		9.90		15.2					0.015	0.003	27.76	M	S	
388.0		10	16	54	20	7	18	9.40	1.54	10.97	M4.5	4.9	13	-6	2	Y	1.178	0.012	28.98	L	P	
394.0		10	27	14	56	15	24	8.69	1.36	8.12	K7	13.0	10	-3	-1	Y	0.029	0.007	28.22	M	P	
398.0		10	33	28	5	22	42	12.61	1.56	11.9	M4 V	13.9	45	-14	-1	O	0.055	0.007	28.56	M	P	
402.0		10	48	19	7	5	6	11.66		12.47	M5 V	6.9	12	-31	-18	O	< 0.011		< 27.27	L	P	
406.0		10	54	6	7	19	12	13.53	2.01	16.65	M8 V	2.4	26	-43	-18	O	0.044	0.005	26.93	ML	P	v
412.0	A	11	3	0	43	46	60	8.77	1.55	10.12	M2	5.4	132	-7	8	O	0.027	0.005	27.13	M	P	
412.0	B	11	3	2	43	46	42	14.45		15.8	M8 V	5.4	132	-7	8	O	0.027	0.005	27.13	M	P	
428.0	A	11	22	29	-61	22	24	7.57	1.26	7.34	K7	11.1	21	-14	-5	Y	< 0.024		< 28.00	L	S	
428.0	B	11	22	29	-61	22	23	8.60		8.37	M0 V	11.1	22	-14	-4	Y	< 0.024		< 28.00	ML	S	
435.0		11	38	37	-44	7	54	7.76	1.07	7.30	K5	12.3	34	-25	4	Y	< 0.008		< 27.63	L	P	
445.0		11	44	35	78	57	42	10.80		12.23	M4 VI	5.2	-71	-59	-77	O	< 0.008		< 26.86	L	P	
447.0		11	45	9	1	6	0	11.10	1.76	13.47	M5 V	3.4	-18	-3	-17	Y	0.017	0.003	26.80	M	P	
447.1	B	11	46	4	14	33	42	10.10		8.68		19.2	9	-5	3	Y	< 0.018		< 28.36	L	S	

TABLE 1—*Continued*

GLIESE number (1)		RA(1950) h	m	s	DEC(1950) d	m	s	m_v (4)	B - V (5)	M_v (6)	Sp (7)	Dist. (pc.) (8)	U	V	W ($Km \cdot s^{-1}$) (9)	Age Flag (10)	Rate $cts\ s^{-1}$ (11)	Error $cts\ s^{-1}$ (12)	log(L_x) $erg\ s^{-1}$ (13)	Rate Flag (14)	Point. Flag (15)	Notes (16)
450.0		11	48	33	35	32	48	9.80		9.71	M1 V	10.4	18	4	0	Y	0.015	0.003	27.75	M	S	
453.0		11	55	27	-27	25	12	6.96	1.16	7.00	K5	9.8	18	-73	-6	O	0.010	0.002	27.51	M	P	
459.3		12	16	56	28	39	30	10.62	1.42	9.20	M2	19.2	51	-23	-32	Y	< 0.005		< 27.78	ML	S	
461.0		12	17	52	0	51	42	10.20		9.09	M0 V	16.7	-4	9	-14	Y	< 0.021		< 28.29	L	S	
471.0		12	28	46	9	5	36	9.78	1.45	8.97	M1 V	14.5	17	-57	5	O	< 0.093		< 28.82	L	S	
473.0	A	12	30	51	9	17	36	13.16	1.80	14.97	M5.5 V	4.3	34	-12	-5	Y	0.039	0.008	27.10	L	P	
473.0	B	12	30	51	9	17	42	13.40		15.22	M7	4.3					0.039	0.008	27.09	L	P	
490.0	A	12	55	19	35	29	48	10.60	1.42	9.01	M0	20.8	12	-27	-7	Y	0.107	0.010	28.90	M	S	h
490.0	B	12	55	18	35	29	36	13.16	1.61	11.57	M4 V	20.8	12	-27	-7	Y	0.107	0.010	28.90	M	S	h
493.1		12	58	5	5	57	6	13.37	1.73	13.87	M5 V	7.9	44	0	-32	O	0.018	0.005	27.58	M	P	
494.0		12	58	19	12	38	42	9.75	1.44	9.55	M2 V	11.0	30	-17	-8	Y	0.257	0.011	29.02	M	P	
509.0	A	13	21	14	29	29	42	9.56	1.33	8.22	M0 V	18.5	47	-9	-33	O	0.007	0.003	27.61	M	S	
509.0	B	13	21	14	29	29	42	9.80		8.46	K6 V	18.5	47	-9	-33	O	0.007	0.003	27.61	M	S	
512.0	A	13	25	46	-2	5	36	11.24	1.52	10.86	M4 V	11.9	-13	-8	-29	O	< 0.012		< 27.77	L	S	
512.0	B	13	25	46	-2	5	36	14.20		13.82	M6 V	11.9	-13	-8	-29	O	< 0.012		< 27.77	L	S	
513.0		13	26	52	11	42	54	13.40		12.10	M5	18.2	-91	-69	5	H	< 0.007		< 27.93	L	S	
514.1		13	27	29	-8	26	36	14.18	1.63	13.03	M6 V	16.9					< 0.011		< 28.03	L	P	
516.0	A	13	30	18	17	4	12	12.00	1.53	10.78	M4 V	17.5	-31	0	0	O	< 0.013		< 28.13	L	S	
516.0	B	13	30	18	17	4	12	12.30		11.08	M4 V	17.5	-31	0	0	O	< 0.013		< 28.13	L	S	
517.0		13	32	7	-8	5	6	9.33	1.18	7.34	K5 V	25.0	29	-20	-17	Y	0.164	0.004	29.54	ML	P	v
527.0	B	13	44	53	17	42	18	10.70		9.48	M2 V	17.5	36	-22	-6	Y	0.116	0.009	28.78	L	P	
528.0	A	13	46	47	27	13	42	7.59	1.12	7.29	K6 V	11.5	18	-21	-14	Y	< 0.010		< 27.64	L	S	
528.0	B	13	46	47	27	13	42	8.03		7.73	K6 V	11.5	18	-21	-15	Y	< 0.010		< 27.64	L	S	
536.0		13	58	31	-2	25	18	9.80		9.62	M0 V	10.9					< 0.010		< 27.60	L	S	
546.0		14	19	48	29	51	42	8.54	1.26	7.73	K8	14.5	24	-54	-19	O	0.006	0.002	27.65	M	P	
548.0	A	14	23	24	23	51	24	9.71	1.41	8.77	M1 V	15.4	-98	-20	-14	O	< 0.019		< 28.19	L	S	
548.0	B	14	23	27	23	51	36	9.97	1.44	9.04	M2 V	15.4	-95	-21	-22	O	< 0.020		< 28.21	L	S	
549.0	B	14	23	29	52	3	42	11.1		10.26	M3.5	14.7	-9	-32	6	O	0.337	0.009	29.40	M	P	
550.1		14	25	31	24	3	48	10.91	1.27	9.41	M0 V	20.0	56	-37	-36	O	< 0.011		< 28.18	L	S	
551.0		14	26	19	-62	28	6	11.05	1.97	15.49	M5 V	1.3	25	-2	13	Y	0.472	0.013	27.43	ML	P	
559.0	B	14	36	11	-60	37	48	1.33	0.88	5.71	K0	1.3	28	1	13	O	0.401	0.010	27.08	L	P	
561.0		14	41	9	26	57	42	9.50		8.08	K0	19.2	43	-39	-61	O	< 0.007		< 27.96	L	S	
566.0	B	14	49	5	19	18	24	6.84	1.00	7.76	K4	6.5	-6	1	1	Y	0.604	0.029	28.64	ML	P	h
567.0		14	51	7	19	21	12	6.04	0.84	5.66	K1	11.9	38	-14	-16	Y	0.081	0.016	28.59	L	P	
569.0		14	52	8	16	18	18	10.20	1.48	10.11	M0 V	10.4	-15	6	-3	Y	0.071	0.010	28.42	L	P	
576.0		15	2	27	5	50	18	9.87	1.30	8.65	K5 V	17.5	47	-65	-44	O	< 0.008		< 27.92	L	P	
581.0		15	16	50	-7	32	24	10.58	1.61	11.50	M5 V	6.5	41	-25	0	Y	< 0.006		< 26.97	L	P	
600.0		15	49	46	11	1	36	9.38	1.40	7.55	M0 V	23.3	-5	-37	9	O	< 0.022		< 28.60	L	S	
615.2	C	16	12	3	33	53	54	12.24		10.51	M V	22.2	10	-32	7	O	< 0.010		< 28.25	L	P	
616.2		16	15	59	55	23	48	9.96	1.46	8.37	M1 V	20.8	-49	-28	-17	O	0.170	0.006	29.40	M	P	
619.0		16	19	12	41	4	36	8.98	1.30	8.58	M0 V	12.0	5	5	4	Y	< 0.005		< 27.38	L	S	
624.1	B	16	23	18	61	37	36	8.80		6.97	K2	23.3	6	-11	-8	Y	< 0.007		< 28.08	ML	P	
628.0		16	27	31	-12	32	18	10.12	1.60	12.08	M5 V	4.0	5	-19	-16	Y	< 0.007		< 26.60	L	P	
629.1		16	30	11	-12	28	60	10.90		9.31	M0 V	20.8					< 0.018		< 28.43	L	S	
643.0		16	52	45	-8	13	54	11.70	1.70	12.73	M4 VI	6.2	-24	-30	12	O	< 0.783	0.028	< 29.01	L	P	h

TABLE 1—*Continued*

GLIESE number (1)		RA(1950) h	m	s (2)	DEC(1950) d	m	s (3)	m_v (4)	B - V (5)	M_v (6)	Sp (7)	Dist. (pc.) (8)	U	V	W ($Km \cdot s^{-1}$) (9)	Age Flag (10)	Rate $cts\ s^{-1}$ (11)	Error $cts\ s^{-1}$ (12)	$\log(L_x)$ $erg\ s^{-1}$ (13)	Rate Flag (14)	Point. Flag (15)	Notes (16)
644.0	A	16	52	48	-8	14	42	9.76	1.62	10.79	M4.5 V	6.2	-22	-30	11	O	0.783	0.028	28.71	L	P	h
644.0	B	16	52	48	-8	14	42	9.80		10.83	M4.5 V	6.2	-22	-30	11	O	0.783	0.028	28.71	L	P	h
644.0	C	16	52	55	-8	18	12	16.66	2.05	17.69		6.2	-21	-30	12	O	< 0.018		< 27.38	L	P	
659.0	A	17	9	8	54	33	24	8.85	1.16	7.35	K8 V	20.0	-12	10	0	Y	0.020	0.004	28.14	ML	S	
659.0	B	17	9	10	54	33	6	9.35	1.26	7.85	K8 V	20.0	-11	3	-8	Y	0.020	0.004	28.14	ML	S	
666.0	B	17	15	15	-46	35	6	8.69	1.41	9.28	M0 V	7.6	-25	19	-26	O	< 0.004		< 26.92	L	P	
669.0	A	17	17	54	26	32	48	11.36	1.55	11.34	M4 V	10.1	32	-14	-1	Y	0.164	0.010	28.46	M	S	h
669.0	B	17	17	53	26	32	48	12.92	1.58	12.90	M5 V	10.1	32	-14	-1	Y	0.164	0.010	28.46	M	S	h
673.0		17	23	16	2	10	12	7.53	1.36	8.15	K7	7.5	0	-52	-9	O	0.016	0.006	27.50	L	P	
675.0		17	25	9	67	20	54	6.43	0.76	5.81	K0	13.3	-2	-51	5	O	< 0.031		< 28.27	L	S	
687.0		17	36	42	68	23	6	9.15	1.50	10.79	M3.5	4.7	-30	-20	-2	O	< 0.012		< 26.95	ML	P	
695.0	B	17	44	28	27	44	42	10.33	1.49	10.80	M4 V	8.1	-15	-30	-5	O	0.014	0.002	27.03	M	P	
695.0	C	17	44	28	27	44	42	10.79		11.26	M4 V	8.1	-15	-30	-5	O	0.014	0.002	27.03	M	P	
699.0		17	55	23	4	33	18	9.54	1.74	13.22	M5	1.8	139	6	19	O	< 0.012		< 26.14	ML	P	
702.0	A	18	2	56	2	30	36	4.22	0.86	5.76	K0	4.9	-6	-18	-18	O	0.222	0.010	27.96	M	P	h
702.0	B	18	2	56	2	30	36	6.00	1.15	7.45	K5 V	5.1	-4	-21	-19	O	0.222	0.010	28.00	M	P	h
719.0		18	32	45	51	40	59	8.30		7.33	M0E V	15.6	-15	-19	-28	O	0.556	0.013	29.67	L	P	
720.0	A	18	33	50	45	41	48	9.86	1.42	9.02	M2 V	14.7	35	-4	-31	O	< 0.005		< 27.60	L	S	
720.0	B	18	33	59	45	42	54	14.00		13.57		12.2					< 0.005		< 27.44	L	S	
724.0		18	38	8	-13	25	6	10.70		9.40	M	18.2					< 0.004		< 27.66	L	S	
725.0	A	18	42	12	59	33	18	8.90	1.54	11.15	M4 V	3.5	25	-2	30	Y	0.020	0.006	26.62	M	P	
725.0	B	18	42	13	59	32	60	9.69	1.59	11.94	M5 V	3.5	24	-2	30	Y	0.020	0.006	26.62	M	P	
729.0		18	46	45	-23	53	30	10.60		13.29	M4.5 V	2.9	5	0	-8	Y	0.163	0.010	27.67	L	P	
735.0		18	53	3	8	20	18	10.11	1.75	9.83	M2 V	11.4	1	-2	-7	Y	0.160	0.007	28.85	L	P	
736.0		18	53	12	4	12	6	8.05	0.90	7.18	K0 V	14.9	-17	6	-1	Y	< 0.005		< 27.59	L	P	
748.2	B	19	12	26	2	4	18	12.00		10.31		21.7					< 0.059		< 28.98	L	S	
752.0	A	19	14	29	5	5	48	9.12	1.50	10.29	M3.5	5.8	-51	-9	-5	O	0.017	0.002	27.25	M	P	h
752.0	B	19	14	32	5	4	42	17.38	2.12	18.55	M5 V	5.8	-51	-9	-8	O	0.017	0.002	26.34	M	P	h
754.1	B	19	17	51	-7	45	18	12.12	1.31	12.16	M5 V	9.8					< 0.008		< 27.41	L	P	
764.0		19	32	28	69	34	36	4.69	0.80	5.92	K0	5.7	-30	43	-18	O	0.045	0.005	27.69	M	P	
765.0	B	19	35	6	50	6	18	13.00		11.74		17.9	22	-27	4	Y	0.058	0.006	28.50	M	P	
766.0	A	19	43	43	27	1	12	12.60		12.47	M4.5 V	10.6					< 0.010		< 27.57	L	S	
766.0	B	19	43	43	27	1	12	13.60		13.47		10.6					< 0.010		< 27.57	L	S	
783.0	A	20	7	55	-36	13	42	5.32	0.87	6.56	K3	5.6	118	-49	48	H	< 0.009		< 26.99	L	P	h
783.0	B	20	7	55	-36	13	42	11.50		12.74	M5 V	5.6	118	-49	48	H	< 0.009		< 26.99	L	P	h
785.0		20	12	10	-27	10	60	5.73	0.88	6.13	K0	8.3	70	-11	-16	O	< 0.010		< 27.36	L	P	
791.2		20	27	21	9	31	12	13.05	1.71	13.32	M6 V	8.8					0.038	0.004	28.01	L	P	
803.0		20	42	4	-31	31	6	8.61	1.44	8.88	M0	8.8	4	-13	-12	Y	2.289	0.059	29.79	L	P	
806.1	B	20	44	5	33	46	48	13.40	1.66	11.67	M4	22.2	51	0	-6	O	< 0.006		< 28.03	L	P	
808.2		20	48	4	29	11	54	8.41	1.06	7.17	K5	17.5	3	-14	-2	Y	0.046	0.013	28.69	ML	S	
812.0	A	20	54	7	-5	2	12	11.87	1.49	10.80	M4 V	16.4	52	-30	-38	Y	0.036	0.003	28.52	M	P	
820.0	A	21	4	40	38	30	0	5.22	1.17	7.56	K5	3.4	90	-53	-8	O	0.085	0.010	27.22	M	P	
820.0	B	21	4	40	38	30	0	6.03	1.37	8.37	K7	3.4	90	-53	-8	O	0.085	0.010	27.22	M	P	
825.0		21	14	20	-39	3	42	6.67	1.38	8.75	M0	3.8	-57	-19	27	O	0.033	0.006	27.22	M	P	
830.0		21	27	16	-12	43	36	9.08	1.29	8.01	M0	16.4	97	-61	-8	O	< 0.013		< 28.08	L	S	

TABLE 1—*Continued*

GLIESE number		RA(1950) h	m	s	DEC(1950) d	m	s	m_v	B - V	M_v	Sp	Dist. (pc.)	U	V	W	Age Flag	Rate $cts\ s^{-1}$	Error $cts\ s^{-1}$	$\log(L_x)$ $erg\ s^{-1}$	Rate Flag	Point. Flag	Notes
(1)		(2)			(3)			(4)	(5)	(6)	(7)	(8)		$(Km \cdot s^{-1})$ (9)		(10)	(11)	(12)	(13)	(14)	(15)	(16)
832.0		21	30	14	-49	13	12	8.67	1.46	10.32	M1	4.7	-5	-18	-2	O	< 0.010		< 26.87	L	P	
845.0		21	59	33	-56	59	36	4.68	1.05	7.00	K5	3.4	77	-38	3	O	0.047	0.004	27.27	M	P	
849.0		22	7	0	-4	53	12	10.42	1.52	10.67	M3 V	8.9	41	-15	-18	Y	0.010	0.003	27.46	M	S	
851.0		22	9	5	18	10	36	10.33		9.93	M2 V	12	29	-32	18	O	< 0.012		< 27.76	L	S	
852.0	A	22	14	42	-9	3	0	13.24		13.22	M4.5 V	10.1	-45	20	-32	O	< 0.033		< 28.07	L	S	
852.0	B	22	14	42	-9	3	0	14.30		14.28	M5 V	10.1	-45	20	-32	O	< 0.033		< 28.07	L	S	
860.0	A	22	26	13	57	26	48	9.85	1.62	11.87	M3 V	4.0	-22	-21	1	O	0.034	0.006	26.96	M	P	
860.0	B	22	26	13	57	26	48	11.30	1.80	13.32	M4.5 V	4.0	-22	-21	1	O	0.034	0.006	26.96	M	P	
862.0		22	26	25	-30	15	48	7.65	1.10	7.05	K5	13.2	-6	-49	-14	O	< 0.021		< 28.08	L	S	
866.0		22	35	45	-15	35	36	12.18	1.96	14.49	M7 V	3.4	69	0	40	O	0.036	0.004	27.16	ML	P	
867.0	A	22	36	1	-20	52	48	9.10	1.49	9.29	M2 V	9.2	19	-9	-2	Y	0.587	0.027	28.93	ML	P	v
867.0	B	22	36	1	-20	52	48	11.45	1.62	11.64	M4 V	9.2	19	-9	-2	Y	0.587	0.027	28.93	ML	P	v
875.0		22	47	43	-7	21	24	9.87		9.13	M1 V	14.1	0	4	12	Y	< 0.005		< 27.52	L	P	
875.1		22	49	30	31	29	24	11.80		10.02	M3.5 V	22.7	34	-14	-23	Y	0.184	0.006	29.51	ML	P	v
879.0		22	53	37	-31	49	48	6.49	1.10	7.03	K5	7.8	4	-7	-14	Y	0.055	0.006	28.06	M	P	
880.0		22	54	10	16	17	24	8.68	1.51	9.50	M2 V	6.8	-32	-11	21	O	0.028	0.004	27.65	M	P	
887.0		23	2	39	-36	8	30	7.36	1.46	9.59	M2	3.6	101	-14	-57	O	0.013	0.004	26.75	M	P	
889.0	A	23	4	26	-23	25	36	9.68	1.34	8.18	M0 V	20.0	-3	-26	-24	O	< 0.015		< 28.31	L	S	
894.0		23	14	51	-42	27	54	10.20		9.16	K5	16.1					< 0.006		< 27.75	L	S	
896.0	A	23	29	20	19	39	42	10.38	1.56	11.33	M4 V	6.5	14	-7	-4	Y	0.531	0.014	28.58	ML	P	v
896.0	B	23	29	20	19	39	42	12.40		13.35	M6 V	6.5	13	-9	-3	Y	0.531	0.014	28.58	ML	P	v
900.0		23	32	26	1	19	42	9.59	1.35	8.44	M1 V	16.9	24	-8	-1	Y	0.055	0.011	28.73	M	S	
905.0		23	39	26	43	55	12	12.29	1.92	14.78	M6 V	3.2	-33	-77	0	O	< 0.008		< 26.44	L	P	
908.0		23	46	36	2	8	12	8.98	1.48	10.26	M2	5.6	8	-64	35	O	< 0.006		< 26.81	L	P	
908.2		23	48	22	19	40	0	17.00		15.50	M5	20.0					< 0.005		< 27.82	L	S	
909.0	A	23	49	57	75	15	54	6.41	0.98	6.25	K3	10.8	14	-6	0	Y	0.064	0.008	28.10	ML	P	
909.0	B	23	49	57	75	15	54	11.70		11.54	M2	10.8	14	-6	0	Y	0.064	0.008	28.10	ML	P	
910.0		23	50	36	28	44	24	9.74	1.39	8.63	M0 V	16.7	-9	7	6	Y	0.011	0.004	28.01	M	S	
1003.0		0	4	46	28	58	48	14.18	1.48	12.84		18.5					< 0.007		< 27.89	L	S	
1055.0		3	6	17	9	50	30	14.86	1.71	14.48		11.9					< 0.010		< 27.67	L	S	
1064.0	A	3	43	37	41	17	24	8.15	0.78	6.46	K1	21.7	88	-99	-71	H	< 0.008		< 28.10	L	P	
1064.0	B	3	43	37	41	17	30	8.74	0.90	7.05	K2	21.7	91	-97	-72	H	< 0.008		< 28.10	L	P	
1151.0		11	48	29	48	40	6	13.26	1.84	13.67		8.3					< 0.005		< 27.07	L	S	
1167.0	A	13	7	13	29	15	12	14.18	1.72	12.84	M5	18.5					0.013	0.002	28.18	M	S	
1193.0		15	32	13	14	26	18	13.83	1.56	12.28		20.4					< 0.009		< 28.10	L	S	
1197.0		16	5	9	26	58	36	13.33	1.64	11.64		21.7					< 0.011		< 28.23	L	S	
1207.0		16	54	26	-4	16	0	12.33	1.59	12.44	M5	9.5					0.138	0.012	28.63	M	S	
1216.0		17	19	26	49	19	12	14.40	1.70	13.29		16.7					< 0.025		< 28.37	L	S	
1225.0		18	17	33	68	32	48	15.38	1.88	14.23		16.9					< 0.020		< 28.29	L	S	
1245.0	A	19	52	16	44	17	30	13.41	1.90	15.03		4.7					0.013	0.003	26.71	M	P	
1245.0	B	19	52	17	44	17	30	13.99	1.98	15.61		4.7					0.013	0.003	26.71	M	P	
1255.0	AB	20	38	3	75	24	60	7.30	0.85	5.66	K0	21.3					0.415	0.006	29.51	M	P	
1255.0	C	20	38	3	75	24	60	10.30		8.66		21.3					0.415	0.006	29.51	M	P	
1258.0		20	41	3	35	19	30	11.50		9.51	M3	25.0	-77	23	-24	O	0.010	0.003	28.34	L	S	
9006.0		0	13	47	15	38	42	15.90		14.17		22.2					< 0.002		< 27.48	L	S	

TABLE 1—*Continued*

GLIESE number (1)		RA(1950) h	m	s (2)	DEC(1950) d	m	s (3)	m_v (4)	B - V (5)	M_v (6)	Sp (7)	Dist. (pc.) (8)	U	V	W ($Km \cdot s^{-1}$) (9)	Age Flag (10)	Rate $cts\ s^{-1}$ (11)	Error $cts\ s^{-1}$ (12)	$\log(L_x)$ $erg\ s^{-1}$ (13)	Rate Flag (14)	Point. Flag (15)	Notes (16)
9067.0	A	1	59	28	3	42	6	10.60		8.77	K5 V	23.3	-71	-8	10	O	< 0.005		< 27.98	L	S	
9067.0	B	1	59	28	3	42	18	12.40		10.57	M2	23.3					< 0.005		< 28.00	L	S	
9073.0	B	2	4	60	0	49	48	10.52	1.24	8.53		25.0					< 0.015		< 28.50	L	S	
9087.0		2	34	9	-3	22	23	8.10	0.95	6.32	K0	22.7					0.019	0.004	28.53	M	S	
9092.0	B	2	37	18	0	3	54	9.00		7.17		23.3					< 0.006		< 28.04	L	S	
9126.0		3	41	21	24	43	5	9.20		7.74	K2	19.6					< 0.005		< 27.84	L	S	
9135.0		3	48	4	23	45	11	11.40		9.62	K6 V	22.7	34	7	-14	O	< 0.008		< 28.15	L	S	
9137.0		3	51	31	-37	11	53	12.80		11.46	K	18.5					< 0.012		< 28.13	L	S	
9158.0		4	31	11	5	17	6	8.00		6.17	K1	23.3					< 0.002		< 27.54	L	S	
9185.0		5	35	24	-62	50	12	9.32	1.12	7.44	K5 V	23.8	28	-13	-18	Y	< 0.025		< 28.69	L	S	
9265.0		8	24	8	29	5	42	9.65	1.12	7.82	K8 V	23.3					< 0.005		< 27.93	L	S	
9281.0	A	8	57	25	16	2	6	9.90		8.48	M0 V	19.2					< 0.009		< 28.05	L	S	
9281.0	B	8	57	25	16	2	6	10.50		9.08		19.2					< 0.009		< 28.04	L	S	
9316.0	B	10	5	33	12	14	30	8.14	0.87	6.20	K1 V	24.4	21	-4	-15	Y	0.015	0.004	28.20	M	P	
9316.0	C	10	5	33	12	14	30	13.50		11.56		24.4					0.015	0.004	28.20	M	P	
9400.0	A	12	13	26	5	55	5	9.46	1.22	8.00	K8 V	19.6	16	-35	33	O	< 0.008		< 28.00	L	P	
9400.0	B	12	13	26	5	55	5	11.00		9.54		19.6					< 0.008		< 28.00	L	P	
9418.0		12	48	5	71	27	36	9.50		7.51	K8	25.0	-19	-78	-46	O	< 0.048		< 29.01	L	S	
9427.0		13	5	15	34	40	5	9.34	1.18	7.88	K8 V	19.6	9	-8	-6	Y	< 0.008		< 28.02	L	S	
9515.0		15	13	15	7	47	42	10.60		8.72	M0 V	23.8					< 0.019		< 28.57	L	S	
9533.0		15	56	32	27	52	41	8.02	0.76	6.24	K0 V	22.7	90	-66	4	O	< 0.012		< 28.33	L	S	
9566.0		16	30	23	3	21	11	9.30		7.36	K1 V	24.4	45	-59	-9	O	0.060	0.010	29.09	L	P	
9584.0	C	17	4	17	54	32	6	13.00		11.22		22.7					0.120	0.006	28.85	ML	P	
9599.0		17	39	45	65	1	30	8.40		6.46	K0	24.4					0.015	0.005	28.47	M	S	
9609.0		17	55	58	4	27	36	9.50		7.51	K5 V	25.0	9	-8	1	Y	< 0.008		< 28.22	L	S	
9615.0	B	18	4	59	9	33	18	14.00		12.01		25.0					< 0.091		< 29.29	L	S	
9628.0		18	30	44	-6	55	54	12.00		10.01	K6	25.0					< 0.008		< 28.23	L	S	
9652.0	A	19	12	29	19	13	30	13.00		11.12	K	23.8					0.069	0.008	28.82	L	S	
9652.0	B	19	12	29	19	12	47	14.40		12.52		23.8					0.069	0.008	28.82	L	S	
9653.0	A	19	17	53	-7	45	36	12.12	1.63	12.21	M3	9.6					< 0.008		< 27.42	L	P	
9707.0	C	20	44	11	33	46	54	13.40	1.66	11.71	M4.0 V	21.7					< 0.007		< 28.03	L	P	
9747.0		21	38	47	53	46	36	16.30		14.52	M4	22.7					< 0.013		< 28.37	L	S	

NOTES.—Summary of the optical and X-ray data of the surveyed stars. Age flag in col. (10) gives the age classification, namely: Y = young disk star, O = old disk star, H = halo population star. Rate flag in col. (14) gives the method used for the count-rate evaluation, namely: L corresponding to REV-1 Local method, M corresponding to REV-1 Map method, ML corresponding to maximum likelihood method (see § 3.3). Pointed flag in col. (15) is S for stars observed serendipitously and P for pointed stars. Notes in col. (16) indicate V stars with evidence of long-term X-ray variability according to the maximum likelihood method adopted (Sciortino & Micela 1992), H stars observed also with the HRI on board the *Einstein Observatory*.

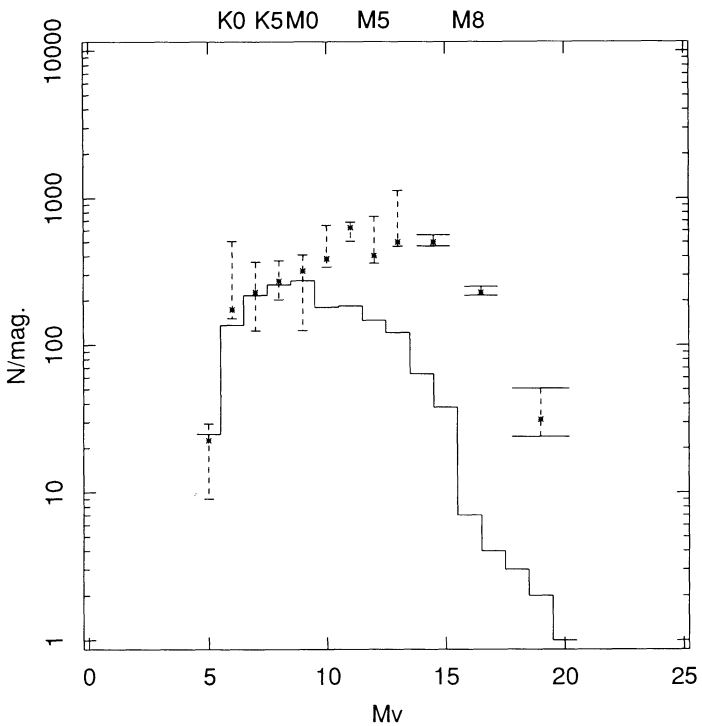

FIG. 3.—Number of stars of our optical sample (expressed in logarithm) per unit magnitude within 25 pc from the Sun (*solid line*) and the expected numbers for a hypothetically complete sample (*asterisks and dashed line bars*).

A P or an S in column (15) of Table 1 denotes whether the star was observed as a result of a direct pointing (P) or serendipitously (S). This distinction, which is important for evaluating the biases of our sample, is worth some discussion. We have first considered as serendipitous those stars whose angular distance from the center of at least one IPC field is greater than 3′. As a check of this choice, we have compared the distribution of stars in young disk, old disk, and halo populations in the optical sample with respect to the same distribution in the serendipitous X-ray sample (see rows 1 and 2 in Table 2). With this choice the subsample of serendipitous K stars presents a statistically significant ($>3\ \sigma$) excess of young stars, with respect to the optical sample. This is due to the fact that members of associations or stellar systems are to be considered pointed stars even if only one of them has been observed as the result of a direct pointing. Hence, the sample of all the originally defined serendipitous stars has to be "cleaned." Among the 131 stars initially considered serendipotous 21 may be considered associated to pointed stars. We have then moved these 21 stars from the serendipitous to the pointed subsample. In Table 2 (row 3) we report the age distribution of stars for the redefined serendipitous sample. The excess of young K stars is not present any more, and the little discrepancy with respect to the optical parent sample is not statistically significant ($<1\ \sigma$).

We have compared the cumulative distance distribution of stars in the optical sample with the one of stars in the whole X-ray sample, separately for the K (Fig. 4*a*) and the M stars (Fig. 4*b*). The two spatial distributions are different at a confidence level greater than 3 σ according to the Kolmogorov-Smirnov (K-S) statistical test. This shows that the X-ray survey has not sampled uniformly in distance the optical sample. In fact, the nearest stars have been preferentially observed as a result of the *Einstein* pointing mode operation. Within ~ 10 pc from the Sun the fraction of stars of the optical sample observed by the *Einstein* satellite is quite high (108 out of 247 $\sim$ 44%), while at greater distances it is of the same order as the *Einstein* sky coverage (149 out of 1434 $\sim$ 10%).

We have split the 25 pc spherical volume in two concentric regions and have investigated for what values of the separation radius the optical and X-ray samples had consistent spatial distributions in the two resulting subvolumes. Using the K-S test we have found that the "best" separating distances are 12 pc for the K stars, and 8 pc for the M stars. In Figure 4 we show the spatial distributions of K (panel c) and M stars (panel d) in these resulting subvolumes.

We have also compared the distributions of the absolute (M_v) and apparent (m_v) visual magnitudes of the optical and X-ray samples, both in the entire volume and in the subvolumes of radius 12 pc (K stars) and 8 pc (M stars). In Table 3 we have reported the results of the K-S test with the null hypothesis that the two compared distributions are extracted from the same parent population. As we can see, the m_v distributions of the K stars in the entire volume within 25 pc from the Sun are different at a confidence level near 3 σ (99.7%), while in the volume of radius 12 pc the confidence level is just slightly above 1 σ (68.3%). Analogously, the M_v distributions of the M stars in the entire volume within 25 pc from the Sun are different at a confidence level greater than 2 σ (95.4%), while in the volume of radius 8 pc the confidence level is well under 1 σ. Hence, with respect to the color distribution, the X-ray samples within the selected radii (12 pc for the K stars and 8pc for the M stars) are statistically indistinguishable from the optical parent population.

In conclusion, the entire X-ray sample represents about 16% of the optical sample, a fraction greater than the sky coverage of the IPC fields (about 10%) due to the presence of a con-

TABLE 2

AGE CLASSIFICATION OF SURVEYED STARS

	K STARS				M STARS			
SAMPLE	Y	O	H	U	Y	O	H	U
Optical	191 (30%)	308 (48%)	16 (2%)	131 (20%)	157 (15%)	241 (23%)	21 (2%)	616 (60%)
Offax >3′	21 (44%)	18 (37%)	1 (2%)	8 (17%)	15 (18%)	25 (30%)	2 (2%)	41 (50%)
Serendipitous	14 (36%)	16 (41%)	1 (3%)	8 (20%)	14 (20%)	17 (24%)	2 (3%)	38 (53%)
Representative	23 (35%)	33 (50%)	2 (3%)	8 (12%)	32 (25%)	47 (37%)	5 (4%)	43 (34%)

NOTES.—Distribution of K and M stars in young disk (Y), old disk (O), halo population (H), and stars with unknown space velocities (U) for the optical sample (row 1), X-ray subsample made of the stars with angular distance from the center of any IPC field greater than 3′ (row 2), redefined X-ray serendipitous sample (row 3), and X-ray representative sample (row 4). The fractions of stars in each age group are given in parentheses.

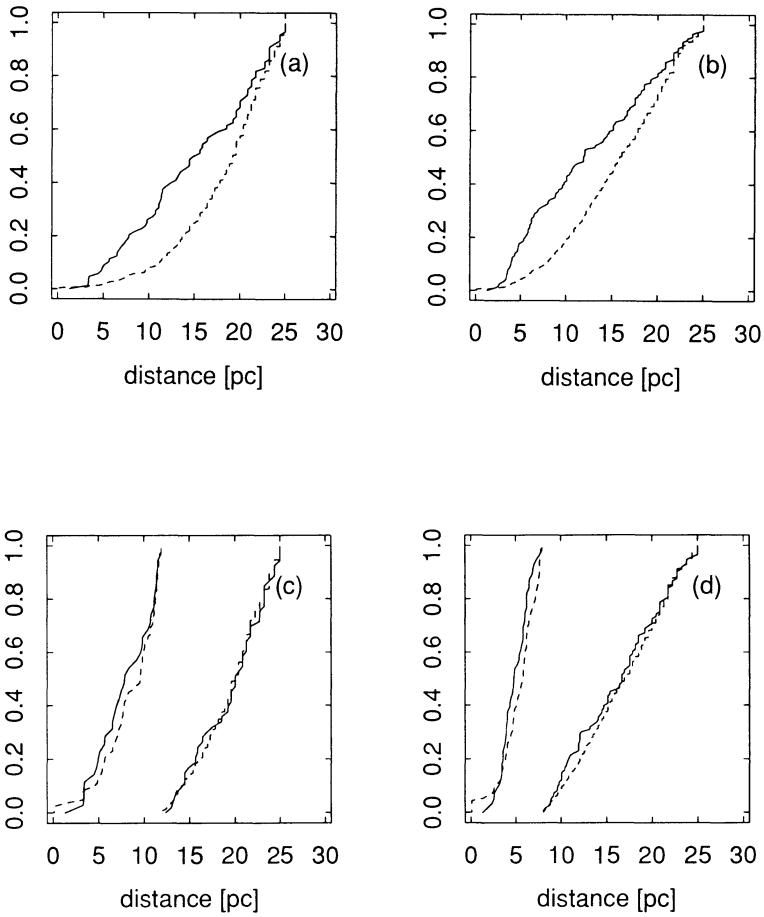

FIG. 4.—Comparison between cumulative distance distributions of stars in the optical sample (*dashed line*) and stars in the X-ray sample separately for the K (*a*) and the M stars (*b*). The same comparison has been performed splitting the entire 25 pc radius spherical volume in two parts using as separating radii 12 pc for K stars (*c*), and 8pc for M stars (*d*).

spicuous number of pointed stars (147 out of 257 stars). The pointed stars, contrary to the serendipitous ones, are affected by selection effects both in their spatial and color distributions. For this reason the entire X-ray sample may not be considered fully representative of the optical parent population. Nevertheless the X-ray subsamples within 12 pc for the K stars and 8 pc for the M stars seem to represent well the optical parent population, at least concerning distance and magnitude distributions.

TABLE 3

COMPARISON OF OPTICAL AND X-RAY SAMPLES IN PROPER SUBVOLUMES

R (pc)	K STARS		M STARS	
	M_v	m_v	M_v	m_v
≤ 25	0.133	0.997	0.978	0.870
≤ 12	0.188	0.696	...	...
≤ 8	...	...	0.396	0.031

NOTES.—Results of the K-S test for the rejection of the hypothesis that the distribution of M_v (m_v) for the stars of the optical and X-ray subsamples are extracted from the same parent population. Three different subsamples are considered: the stars within the entire volume of 25 pc radius, within 12 pc (only for the K stars), and within 8 pc (only for the M stars).

3. DATA REDUCTION

3.1. *Source Detection*

In this work, we have used all the available *Einstein Observatory* Imaging Proportional Counter (IPC) (Gorenstein, Harnden, & Fabricant 1981) data homogeneously reduced with the latest processing (Harnden et al. 1984). They include detections of about 16,000 X-ray sources, and 3 σ upper limits in the 0.16–3.5 keV measured for 30,000 stars contained in the *Einstein Master List Catalogue* (Harris et al. 1990). To search for the X-ray counterparts of the stars of our optical sample which fall in at least one IPC field, we have carried out a positional matching (within 2′) between the positions of the X-ray-detected sources in the *Einstein* broad energy band (0.16–3.5 keV) and the position of our stars, corrected for proper motion displacement. We have found 139 X-ray detections which have as counterpart a star (or a multiple system) of the optical sample. More than 50% of these detections are closer than 30″ to the optical counterpart, and only 20% lie within 1′ and 2′.

Analogously, we have carried out a positional matching between the stars of the optical sample and the 30,000 REV-1

upper limits, and have found 118 more matchings. More than 50% of these upper limits are closer than 12″ to the optical counterpart, only 20% lie within 30″ and 1′, while no upper limits are found further than 1′. In summary, the whole X-ray sample contains 139 X-ray sources, and 118 for which an X-ray upper limit has been estimated in the same *broad* energy band (0.16–3.5 keV).

3.2. *Spurious Sources*

In the standard REV-1 source detection algorithm, the detection threshold (expressed in terms of signal-to-noise ratio) has been chosen so that no more than 0.3 spurious detections can be expected, on average, for each detection algorithm (*LOCAL* or *MAP*) and each energy band (*soft*, *hard*, *broad*) in any field. Since we have retained X-ray sources detected in the *broad* energy band both with the *MAP* the *LOCAL* detection algorithms, we expect, on average, 0.6 spurious detections per field. The mean number of spurious detections in our X-ray sample (n_s) can be expressed as follows:

$$n_s = 0.6 \frac{(S_{\rm obj})}{(S_{\rm IPC})} (N_{\rm obj}) = 0.6\ 3.5 \times 10^{-3}\ 257 = 0.54\ ,$$

where $S_{\rm obj}$ is the area of the allowed acceptance circle (2′ radius), $S_{\rm IPC}$ is the area of an IPC field (60′ × 60′), and $N_{\rm obj}$ is the number of objects of the X-ray sample.

We have also to consider the possibility of chance coincidence between the stars of our X-ray sample and other stellar or extragalactic X-ray sources.

Using the current available stellar X-ray luminosity functions of stars of different spectral types, the mean limiting sensitivity of each IPC field, and adopting a detailed model of stellar coronal component of the galaxy (Favata, Micela, & Sciortino 1992), we have estimated that 54 stellar sources of spectral types different from K or M may be detectable within the 185 IPC fields of our survey. In a similar way, we have used the Extended Medium Sensitivity Survey results of Gioia et al. (1989) and have estimated that 101 extragalactic sources (largely AGNs) may be detectable in the fraction of sky covered by our survey. Assuming that these sources are uniformly scattered in the survey area we expect a mean number of (54 + 101)/185 = 0.84 sources per field, and therefore the number of possible chance coincidences (n_c) with our stars are

$$n_c = 0.84 \frac{(S_{\rm obj})}{(S_{\rm IPC})} (N_{\rm obj}) = 0.84\ 3.5 \times 10^{-3}\ 257 = 0.75\ .$$

The total number of possible mistaken identifications among the stars of our X-ray sample is therefore 1.29.

3.3. *Count Rate Determination*

In passing from counts collected in the detection and in the background cells to source count rate, REV-1 data processing applies three corrections to take into account (1) vignetting, (2) the IPC point response function, and (3) photon scattering due to mirror imperfections.

The mirror-detector assembly tends to scatter soft photons more than hard ones; for this reason, the point response function of a hard source is sharper than that of a soft source. Considering that the point response function correction used in REV-1 has been evaluated assuming an emission spectrum typical of an extragalactic object (harder than a stellar one), we had to introduce a further correction to compute the count rate for stellar sources. We have considered 85 detected stars of our sample, unobscured by detector support structure and edges, and have computed the further correction factor as the trimmed average (excluding 5% tails) of the fraction between the count rate in a 3′ radius cell and the count rate in the detection cell (2.′4 × 2.′4). The further correction factor we have found (1.419) has been applied to calculate the count rates both for the detections and the upper limits. Previous stellar surveys had derived and adopted correction factors for other spectral types: 1.14 for the O stars (Chlebowski, Harnden, & Sciortino 1989), 1.14 for the B stars (Grillo et al. 1992), 1.25 for the G stars (Maggio et al. 1987). The correction factor for K and M stars is therefore the highest, suggesting that low-mass stars have the softest X-ray spectrum among all stars.

As the best estimate of the quiescent X-ray emission level of stars observed in more than one IPC field (41 stars) we have adopted the *maximum likelihood* ML count rate of Sciortino & Micela (1992).

When different observations of a star are all upper limits, their merging could result into a detection (i.e., the resulting S/N ratio becomes greater than 3, the chosen threshold for detection). When this is the case, we adopt the ML count rate, otherwise the lowest upper limit. Applying the variability technique of Sciortino & Micela (1992) we have searched for the occurrence of variations with respect to the ML count rate with a significance greater than 3 σ. Among the 41 stars with multiple observations, 11 show evidence of variability (see notes in Table 1). A more detailed account of the variability study will be presented elsewhere. Here we note only that no variations larger than a factor ~ 2 have been detected between two observations.

3.4. *Count Rate to Flux Conversion*

The conversion factor from count rate to X-ray flux in the broad band (0.16–3.5 keV), depends on instrumental properties, the hydrogen column density along the line of sight, and the assumed source spectrum. Vaiana et al. (1981), assuming a single temperature Raymond-Smith spectrum of a few million degrees, and negligible hydrogen column densities, have determined a conversion factor of 2×10^{-11} ergs cm^{-2} counts^{-1} per IPC count in the broad band.

In a recent study of stellar X-ray spectra based on a sample of 130 stars with more than 200 counts, Schmitt et al. (1990b) have shown that the X-ray spectra of a sizable fraction of late-type stars are better described by a two temperature model. Considering the 20 K and M stars of our sample which are contained in the sample of Schmitt et al. (1990b), we have studied the distribution of the a posteriori conversion factors derived if the X-ray flux is computed with a two temperature model description. This distribution is symmetrical around the mean value of 1.95×10^{-11} ergs cm^{-2} counts^{-1} and has a width of approximately 15% of the mean value. This result is therefore consistent with the standard conversion factor of 2×10^{-11} ergs cm^{-2} counts^{-1}, that we use in this work.

3.5. *Multiple Counterparts*

There are 44 cases where the same X-ray source has more than a single star as possible optical counterpart. In these cases we have adopted the following criteria:

1. When more than one late-type star (F, G, K, and M spectral types) is in the error circle, the X-ray luminosity has been divided in equal parts among the possible counterparts.
2. When an A type star and/or a white dwarf is in the error

circle, these have been assumed not to contribute to the X-ray source.

We compared on a statistical basis the X-ray luminosity function of the sources with single optical counterparts and the X-ray luminosity function of the sources whose X-ray luminosity has been derived according to the above rules. The two luminosity functions are statistically indistinguishable confirming the reliability of the adopted solution.

Of course, whenever high-resolution observations were available (notes in Table 1 indicate stars which have been observed also with the High Resolution Imager) we have used the additional information. In HRI sequence 3838 the star Gliese 166 C is about 3 times brighter than Gliese 166 A, and we have accordingly split the measured IPC X-ray flux. In HRI sequence 4390 the star Gliese 643 can be resolved from the binary system Gliese 644 A and B (the three stars are not resolved by the IPC), but no X-ray flux is measured on the position of Gliese 643. Hence we have attributed to the two stars Gliese 644 A and B half of the total IPC X-ray flux and have considered Gliese 643 as an upper limit equal to the total X-ray flux of the IPC detection. In HRI sequence 5627 the star Gliese 752 A is 8 times brighter than Gliese 752 B, and we have accordingly split the measured IPC X-ray flux.

3.6. *Comparison with Previously Determined L_X*

Values of the X-ray luminosities based on the *Einstein Observatory* data have been previously reported for a large sample of K and M stars (Bookbinder 1985), using a preliminary version of the IPC data reduction system. The final standard processing system (REV-1) of the IPC data (Harnden et al. 1984) properly incorporates all instrumental characteristics in evaluating source net counts from IPC X-ray images; it evaluates for each IPC sequence the temporal and spatial dependence of the instrumental gain, this obtaining better estimates of the background; it adopts an improved detection algorithm, which is less likely to detect spurious sources in regions of high background. It is therefore interesting to compare the X-ray luminosities derived by us with those pre–REV-1.

In Figure 5 we plot our X-ray luminosities (vertical axis) versus the X-ray luminosities reported by Bookbinder (1985). We notice a dispersion of a factor ~ 3 in X-ray luminosity, with the exception of few cases where the two values differ by an order of magnitude. Most of the systematic shift between the two determinations is due to the different recipe adopted to estimate X-ray luminosities of members of multiple system being counterparts of the same X-ray source. However, if we consider only those X-ray sources with a single optical counterpart, a systematic effect still remains which is likely due mainly to the better background evaluation.

4. RESULTS

In Figure 6 we show the X-ray luminosity dependence on distance for the entire X-ray sample. The solid lines represent, from bottom to top, the X-ray luminosity threshold corresponding to X-ray flux sensitivity limits of 10^{-13}, 10^{-12}, and 10^{-11} ergs s^{-1} cm^{-2}. We notice that (1) faint objects are not present at great distance because of the limit sensitivity of the IPC, and (2) the lack of luminous objects at distance closer than ~ 5 pc is easily explained if one considers that the volume inside 5 pc is 1/125 of the entire volume inside 25 pc and the luminous objects are only a small percentage of the entire

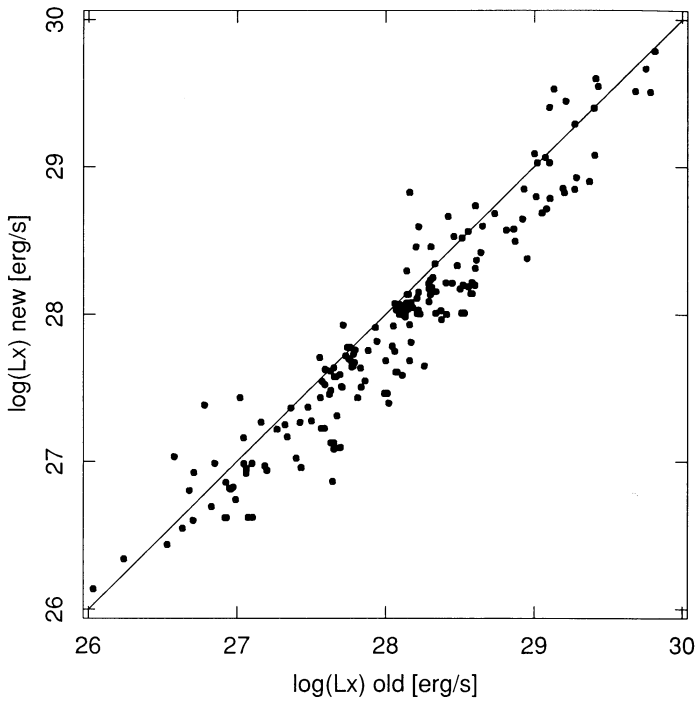

FIG. 5.—log (L_X) in our survey vs. log (L_X) as estimated in a previous survey (Bookbinder 1985) for a common sample of ~ 200 stars. Both detections and upper limits are retained in the comparison.

X-ray sample, unlikely to be present in a small region of space. This means that, for building a truly representative sample, it is necessary also to include X-ray data from more distant stars. We will show in the following how we have accomplished this objective.

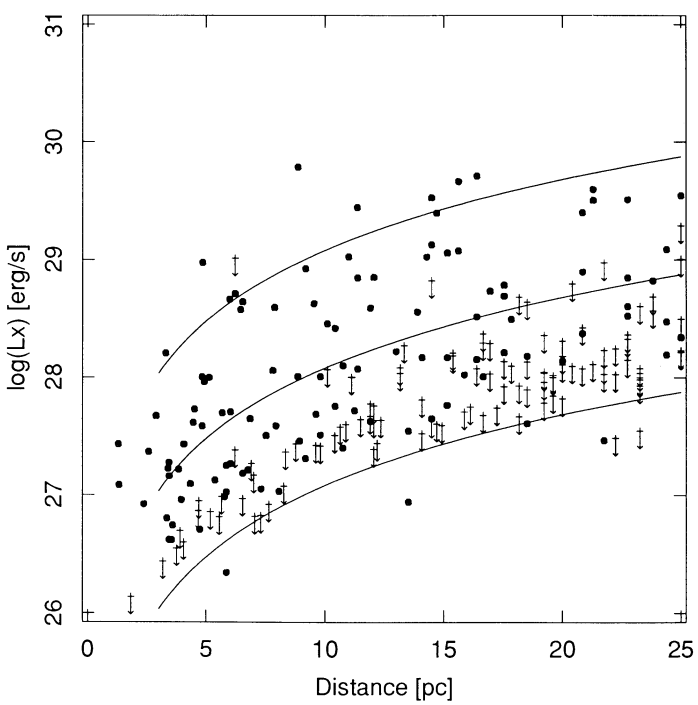

FIG. 6.—X-ray luminosity vs. distance for the entire sample. *Solid dots*: detections; *arrows*: upper limits. Curves, from bottom to top, correspond to the X-ray flux thresholds of 10^{-13}, 10^{-12}, and 10^{-11} ergs s^{-1} cm^{-2}.

4.1. *The Representative X-Ray Sample*

As described in § 2.2, the K stars within 12 pc and the M stars within 8 pc from the Sun may be considered representative of the optical parent sample. In order to investigate whether at least some of the stars at greater distances could also be considered representative, we have compared the cumulative X-ray luminosity function of the closer and representative stars with that of serendipitous stars at greater distances, and also with that of pointed stars at greater distances, separately for the K and M stars.[3] We have found that we cannot reject, at a significance level above 1 σ (43.9% for the K stars and 61.2% for the M stars), the null hypothesis that the X-ray luminosity functions of the near stars and of the serendipitous stars at larger distances are drawn from the same parent population. On the contrary, the X-ray luminosity functions of the near stars and of the pointed stars at larger distances are different with high significance level (96.5% for the K stars and 99.9% for the M stars).

Taking into account these results and the other evidence presented in § 2.2 we are confident that the best available X-ray subsamples are all K stars inside 12 pc plus serendipitous K stars between 12 and 25 pc, and all M stars inside 8 pc plus serendipitous M stars between 8 and 25 pc. In the following we indicate the samples just defined as the "*representative X-ray samples.*"

In Table 2 (fourth row) we have reported the number of stars of the representative X-ray samples in different age groups. The distribution of the representative X-ray sample among the three age groups is consistent with that of the optical parent population.

4.2. *X-Ray Luminosity Functions*

The X-ray cumulative luminosity functions of the representative X-ray sample for the K and M stars are shown in Figure 7. The corresponding means (computed via bootstrap) with 1 σ confidence level uncertainties are

$$\text{K stars: } \langle \log (L_X) \rangle = 27.7 \pm 0.1 \text{ [ergs s}^{-1}\text{]} ,$$

$$\text{M stars: } \langle \log (L_X) \rangle = 27.2 \pm 0.1 \text{ [ergs s}^{-1}\text{]} .$$

A comparison of these two X-ray luminosity functions based on a two-sample Wilcoxon test results in a confidence level equal to 99.9% to reject the null hypothesis that the two samples are extracted from the same parent population; hence we conclude that the two functions are different.

The X-ray luminosities of M stars cover a range of about three orders of magnitude from log $(L_X) \sim 26$ to log $(L_X) \sim 29$ ergs s^{-1}. The X-ray luminosity of K stars ranges between log $(L_X) \sim 27$ and log $(L_X) \sim 29.5$ ergs s^{-1}, and therefore our sample does not contain any star with log $(L_X) < 27$ ergs s^{-1}, in analogy to what has been found for G stars (Maggio et al. 1987). As shown in Figure 6, stars fainter than log $(L_X) = 27$ ergs s^{-1} may be detected only at distance less than ~ 10 pc where the X-ray sample contains only 24 K stars. If the low-luminosity tail of the K stars were the same as that of the M stars ($\sim 40\%$ of M stars are fainter than log $(L_X) = 27$ ergs s^{-1}), then about 10 K stars should have been detected with log $(L_X) \leq 27$ ergs s^{-1}. This evidence suggests that if K stars with log $(L_X) < 27$ ergs s^{-1} do exist, they represent only a very small fraction of the entire population of K stars, which is not the case for the M stars.

[3] We have used the generalized Wilcoxon-Peto-Prentice two-sample test (Schmitt 1985; Feigelson & Nelson 1985) which is more reliable than the Wilcoxon two sample test in comparing samples with different distance distributions hence with different X-ray luminosity threshold distributions.

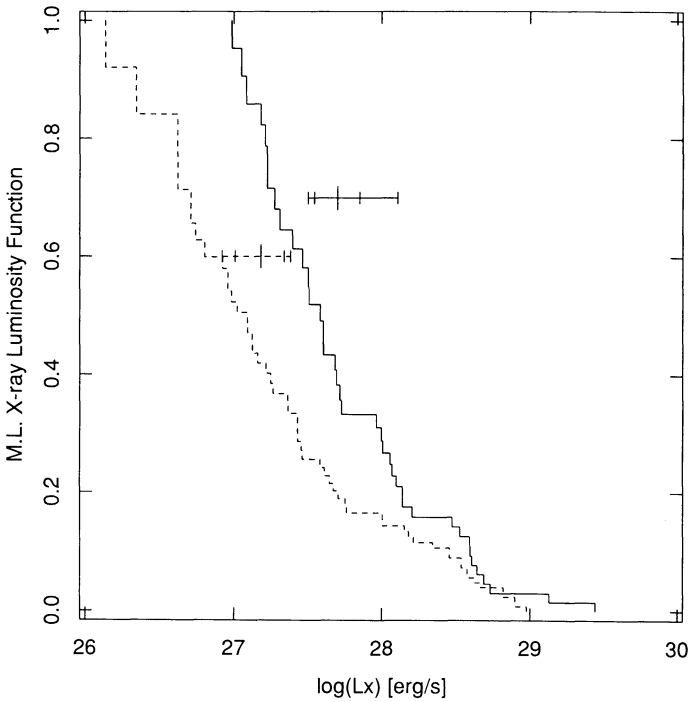

FIG. 7.—X-ray cumulative luminosity functions for the representative samples of K stars (*solid line*) and M stars (*dashed line*). The corresponding means are plotted with 2 and 3 σ confidence level uncertainties.

4.3. *Dependence of X-Ray Luminosity on Spectral Type*

Indications that stars later than M5 present a drop in X-ray emission level have been previously presented for samples of somewhat smaller size (Golub 1983; Bookbinder 1985; Rosner et al. 1985). We have reconsidered this problem with our larger size, less biased, and statistically representative X-ray sample of M stars in the solar neighborhood.

In Figure 8 where we have plotted log (L_X) versus M_v for the representative sample of K and M stars, we note the steep drop in X-ray luminosity at $M_v \sim 13.4$ (dashed vertical line). As we have discussed in § 2.1, the optical sample is severely incomplete at faint magnitudes, and therefore it could be argued that the available sample of late M stars is too small to allow the detection of very bright X-ray sources, which usually represent only a small fraction of the entire population. To investigate whether this is the case or the observed drop is instead a real effect, we have proceeded as follows. We have assumed as a working hypothesis that the M stars later than $M_v = 13.4$ (31 stars) have the same X-ray luminosity function as the earlier M stars. Under this hypothesis, we have evaluated the number of expected detections of late M stars above three given log (L_X) thresholds, namely, 27.5, 28.0, and 28.5 ergs s^{-1}, and we have compared predicted and actual number of detections. We summarize the results of this analysis in Table 4A. The listed probability levels give the significance to which we can reject the hypothesis that the observed number of detections is extracted from a Poisson distribution with mean equal to the predicted number of detections. As we can see, the actual number of detected late M stars is lower than the predicted one at a high confidence level. This result shows that the number of late

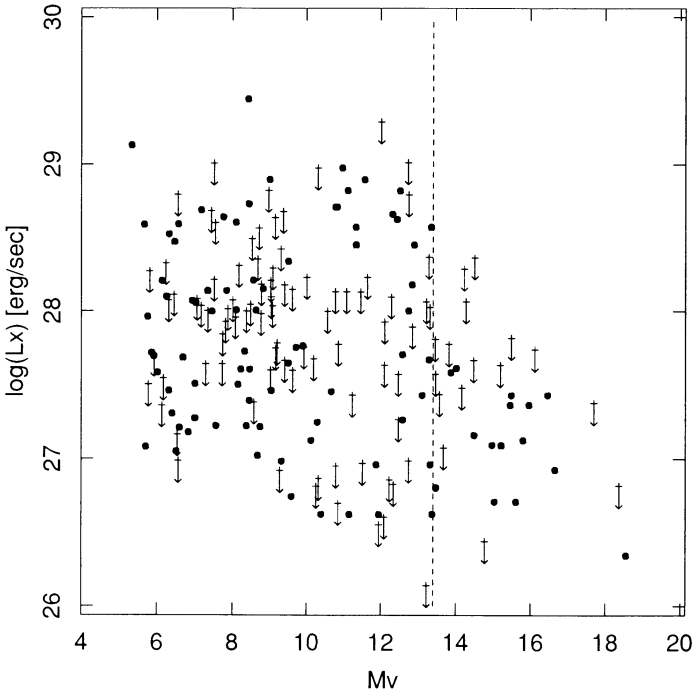

FIG. 8.—X-ray luminosity versus absolute visual magnitude for K and M stars of the representative X-ray sample. *Solid dots*: detections; *arrows*: upper limits; the vertical dashed line corresponds to $M_v = 13.4$.

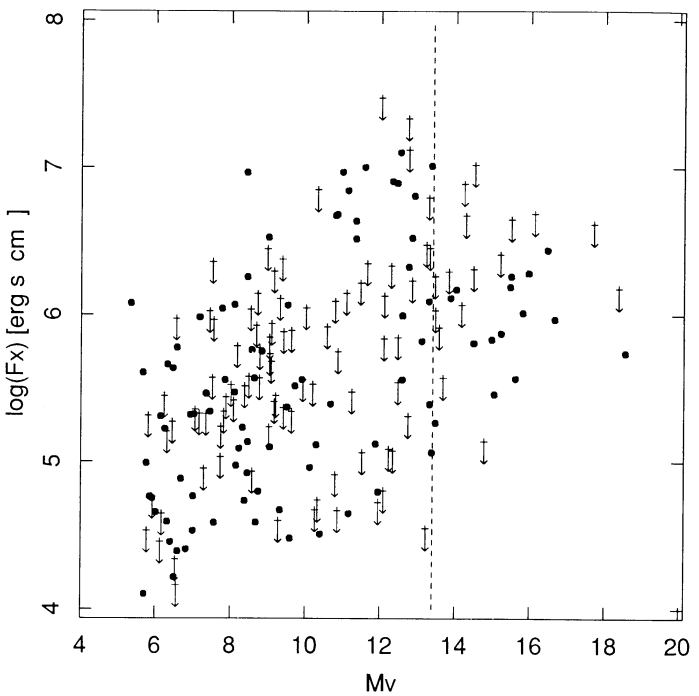

FIG. 9.—X-ray surface flux vs. absolute visual magnitude for K and M stars of the representative X-ray sample. *Solid dots*: detections; *arrows*: upper limits; and the vertical dashed line corresponds to $M_v = 13.4$.

M stars in the representative X-ray sample is large enough to allow the detection of some luminous X-ray sources (log $(L_X) \geq 28$ ergs s^{-1}) if they really existed. For this reason we are confident that the observed drop in X-ray luminosity is real.

TABLE 4

EXPECTATIONS FOR LATE M DETECTIONS

A. X-RAY LUMINOSITY

log (L_X) (ergs s^{-1})	Expected Detections	Observed Detections	Confidence Level
27.5.....	9	2	0.995
28.0.....	7	0	0.999
28.5.....	3	0	0.950

B. X-RAY SURFACE FLUX THRESHOLDS

log (F_X) (ergs s^{-1} cm^{-2})	Expected Detections	Observed Detections	Confidence Level
6.4.....	5	1	0.966
6.6.....	5	0	0.993
6.8.....	3	0	0.950

NOTES.—Table 4A gives statistical results testing the working hypothesis that late M stars follow the same cumulative X-ray luminosity function of early M stars. Col. (1): chosen X-ray luminosity threshold, col. (2): number of late M detections expected over the X-ray luminosity threshold, col. (3): actual number of detected late M stars over the same threshold, and col. (4): confidence level for the rejection of the hypothesis that the actual number of detections is extracted from a Poisson distribution with mean equal to the expected number. Table 4B is analogous to Table 4A but using stellar X-ray surface flux thresholds instead of X-ray luminosity.

Since the late M stars have very small radii, it could be argued that the drop in X-ray luminosity reflects simply the decreasing stellar surface. To investigate this point we have repeated our analysis considering the X-ray surface flux (F_X) instead of the X-ray luminosity (L_X). In Figure 9 we have plotted the stellar X-ray surface flux[4] as a function of absolute visual magnitude for K and M stars of the representative X-ray sample.

The surface X-ray flux increases from the K stars up to the early M stars (as expected since X-ray luminosity is nearly constant), and a change of tendency occurs at nearly $M_v = 13.4$. To evaluate the significance of the observed drop at $M_v = 13.4$ we have applied the same technique adopted for the case of the X-ray luminosity. Table 4B shows that even considering X-ray surface flux, a drop in X-ray emission level for $M_v > 13.4$ is present although the statistical significance is lower.

This result is based on the hypothesis that the optical parent sample we started with is representative of the population of late M stars in the solar neighborhood, despite the observed severe incompleteness discussed in § 2. With regard to this point, we notice that there is no reason why the spatial incompleteness should introduce a selection effect biasing the X-ray representative sample in such a way to select preferentially stars with lower level of X-ray emission. On the contrary, we expect that the composition of the original optical catalog would preferentially include active (i.e., flaring) stars that should have also a high level of X-ray emission (optical flaring is a way to pick up a faint star between the many other of similar magnitude).

[4] Stellar radii have been derived by linear regression between log (R) and log (L_{bol}) from the data presented in Fig. 5 of Pettersen (1982).

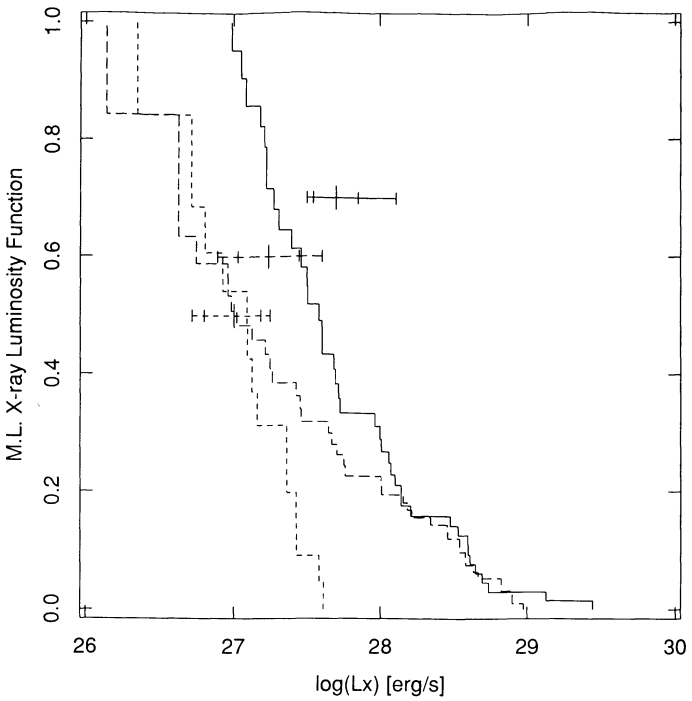

FIG. 10.—X-ray cumulative luminosity functions for the representative samples of K (*solid line*), early M (*long dashed line*), and late M stars (*short dashed line*). The corresponding means are shown with 2 and 3 σ confidence level uncertainties.

Having confirmed the reality of the drop of X-ray luminosity at $M_v \sim 13.4$ we have subdivided the M star sample into two subsamples, early M ($8.5 < M_v \leq 13.4$) and late M ($M_v > 13.4$) stars, respectively. In Figure 10 we show the X-ray cumulative luminosity functions of K, early M, and late M stars. The logarithm of the mean values of the X-ray luminosity with 1 σ confidence level uncertainties are

$$\text{K stars:} \quad \langle \log (L_X) \rangle = 27.7 \pm 0.1 \text{ [ergs s}^{-1}\text{]}$$

$$\text{early M stars:} \quad \langle \log (L_X) \rangle = 27.2 \pm 0.1 \text{ [ergs s}^{-1}\text{]}$$

$$\text{late M stars:} \quad \langle \log (L_X) \rangle = 27.0 \pm 0.1 \text{ [ergs s}^{-1}\text{]} .$$

We may observe that early and late M stars are quite similar in the low-luminosity range while their high-luminosity tails, as expected, are very different from each other. We have compared the X-ray luminosity functions of the above M stars subsamples adopting a two-sample Wilcoxon test. We can reject the null hypothesis that the two samples are extracted from the same parent population to a quite low (90.5%) confidence level. This is likely due to the small number of detections (15) present in the sample of late M stars. We have also compared the X-ray luminosity function of the K stars with the X-ray luminosity functions of the two M star subsamples and we have found confidence levels of 98.6% (K–early M) and, 99.9% (K–late M), respectively.

4.4. *Dependence of X-Ray Luminosity on Age*

There is clear evidence that age plays a fundamental role in accounting for the wide spread in X-ray luminosity of late-type stars (Stern et al. 1981; Caillault & Helfand 1985; Micela et al. 1985, 1988, 1990; Feigelson & Kriss 1989; Schmitt et al. 1990a). We have built X-ray cumulative luminosity functions of young and old disk stars of the representative sample separately for K, early M, and late M stars (see Fig. 11). The derived mean values of log (L_X) with associated 1 σ confidence level uncertainties are listed in Table 5.

TABLE 5

X-RAY LUMINOSITY OF YOUNG AND OLD DISK POPULATIONS

Spectral Type	log (L_X) Young-Disk	ergs s^{-1} Old-Disk
K	28.0 ± 0.1	27.5 ± 0.1
Early M	27.7 ± 0.1	27.0 ± 0.2
Late M	27.3 ± 0.1	26.9 ± 0.2

NOTES.—Means and 1 σ confidence level uncertainties derived from the X-ray luminosity functions of the young-disk and old-disk star subsamples, of the three spectral types, K, early M, and late M, respectively.

The mean of log (L_X) is systematically higher for the young stars, even for late M stars. The Wilcoxon two-sample test comparing the X-ray cumulative luminosity functions of young and old starws in each of the three spectral ranges K, early M, and late M yields the following confidence levels 0.998, 0.999, 0.799, respectively. For the K and early M stars the hypothesis that the X-ray luminosity functions of young and old stars are extracted from the same parent population can be rejected at a confidence level above 3 σ. For the late M stars although the mean of log (L_X) decreases going from young to old stars, the statistical significance for the rejection of the above hypothesis is only above 1 σ level. This is likely due to the quite small size of the two compared subsamples.

To investigate if this result is dependent on the method adopted to separate stars in young and old disk populations (see § 2), we have considered two other kinematical methods of age classification, reported in the literature. According to the first method, young disk stars have an absolute value of the W velocity component (orthogonal to the disk of the Galaxy), with respect to the local standard of rest, smaller than 15 km s^{-1}, while for the old disk stars $|W|$ is greater than 15 km s^{-1} ($|W|$ method, Upgren 1978). According to the second method young disk stars have a peculiar velocity $[V_{pec} = (U^2 + V^2 + W^2)^{1/2}]$ smaller than 30 km s^{-1}, while old disk stars have a peculiar velocity greater than 30 km s^{-1} (V_{pec} method, Meusinger, Reinmann, & Stecklum 1991). We have chosen the cutoff at 30 km s^{-1} in order to obtain a ratio between the numbers of young and old stars consistent with the other two methods.

We have built X-ray luminosity functions of young and old stars for the K, early M, and late M stars using both these two other methods. In Table 6 we report the results of the Wilcoxon two-sample test comparing the X-ray luminosity function of young and old disk stars in the three spectral type ranges considered according to the three different methods of stellar age classification. The Eggen and V_{pec} methods give comparable test results, while the $|W|$ method does not seem to work equally well in separating young and old disk stars if we assume the X-ray luminosity level as an independent criterion. It is worth noting that the $|W|$ method, being based on only one component of stellar velocity, is intrinsically more sensitive to random fluctuations and therefore less reliable than the other two methods. The good accord of the first two methods confirms our result of X-ray luminosity dependence

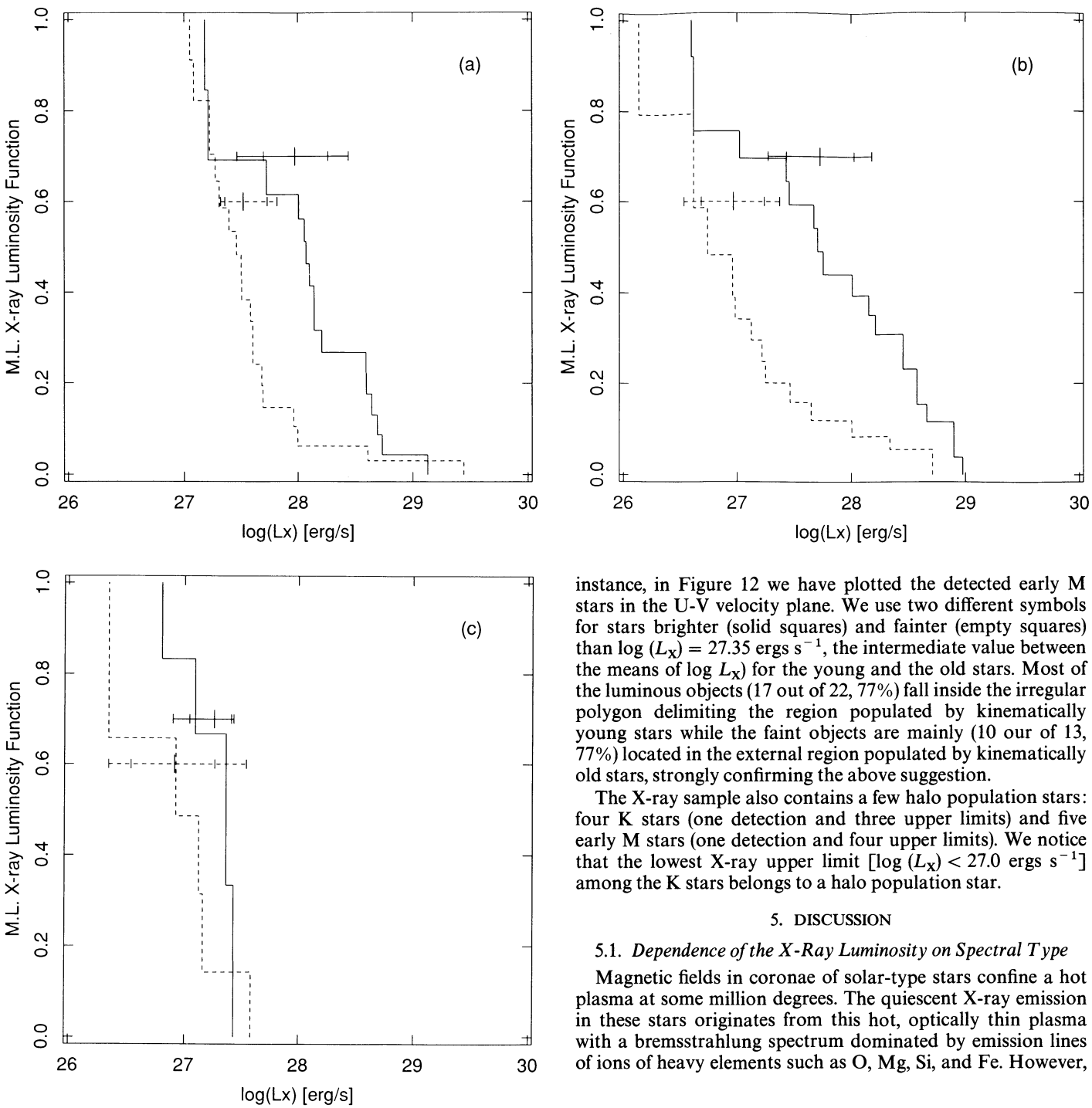

FIG. 11.—X-ray cumulative luminosity functions for young (*solid line*) and old stars (*dashed line*); panel (*a*) for K stars, panel (*b*) for early M stars, and panel (*c*) for late M stars. The corresponding means are shown with 2 and 3 σ confidence level uncertainties.

on age for disk population stars, that is, in the range of ages between $10^{8.5}$ and 10^{10} yr.

This result suggests that the X-ray luminosity level of late-type stars may be used, by itself, to statistically separate a large sample of stars into young and old disk populations with nearly the same accuracy as known kinematical methods. For instance, in Figure 12 we have plotted the detected early M stars in the U-V velocity plane. We use two different symbols for stars brighter (solid squares) and fainter (empty squares) than log (L_X) = 27.35 ergs s^{-1}, the intermediate value between the means of log L_X) for the young and the old stars. Most of the luminous objects (17 out of 22, 77%) fall inside the irregular polygon delimiting the region populated by kinematically young stars while the faint objects are mainly (10 our of 13, 77%) located in the external region populated by kinematically old stars, strongly confirming the above suggestion.

The X-ray sample also contains a few halo population stars: four K stars (one detection and three upper limits) and five early M stars (one detection and four upper limits). We notice that the lowest X-ray upper limit [log (L_X) < 27.0 ergs s^{-1}] among the K stars belongs to a halo population star.

5. DISCUSSION

5.1. *Dependence of the X-Ray Luminosity on Spectral Type*

Magnetic fields in coronae of solar-type stars confine a hot plasma at some million degrees. The quiescent X-ray emission in these stars originates from this hot, optically thin plasma with a bremsstrahlung spectrum dominated by emission lines of ions of heavy elements such as O, Mg, Si, and Fe. However,

TABLE 6

COMPARISON AMONG THREE DIFFERENT STELLAR AGE-CLASSIFICATION METHODS

Method	K	Early M	Late M
Eggen	0.998	0.999	0.799
V_{pec}	0.995	0.999	0.833
$\|W\|$	0.828	0.943	0.853

NOTES.—Wilcoxon two-sample test results for the comparison of young and old disk stars according to three different methods of age classification: the Eggen (U-V polygon), the $|W|$, and the V_{pec} methods (§ 4.4).

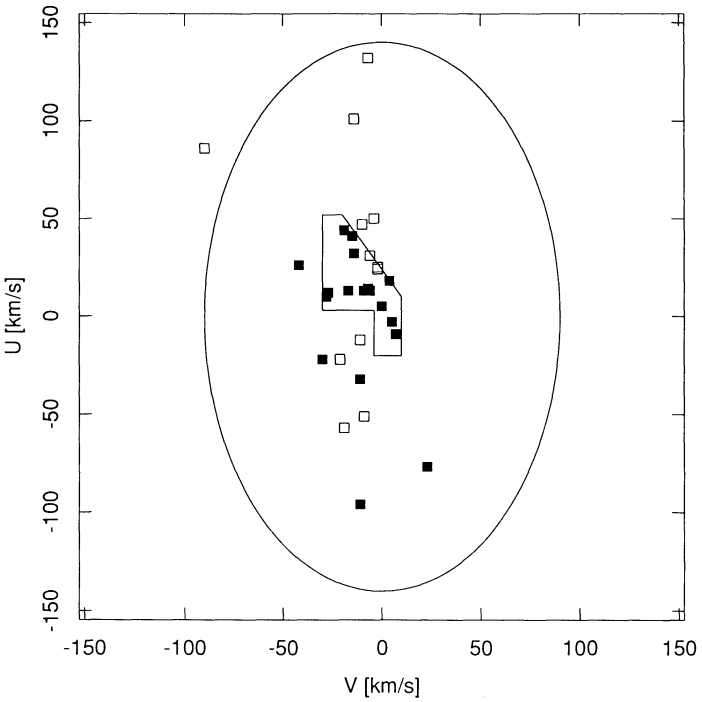

FIG. 12.—Scatter plot of early M stars *U-V* velocity space components. Symbols indicate stars brighter (*solid squares*) or fainter (*empty squares*) than $\log (L_X) = 27.35$ ergs s^{-1}, respectively. Superposed is the polygon indicating the locus of *U-V* velocity components of young stars. The enhancement of bright X-ray stars inside this region is evident.

primordial magnetic fields are not sufficient, mainly because they are not self-sustaining, and the presence of strong magnetic fields in the corona is generally explained through a mechanism of stellar dynamo (Parker 1979).

Our data have allowed us to state the occurrence of a steep drop in X-ray emission for stars later than absolute visual magnitude ~ 13.4, the region where stellar interior models predict the stars to become fully convective. This result, as previously suggested (Golub 1983; Rosner et al. 1985; Bookbinder 1985), indicates the loss of efficiency for the "shell"-type dynamo. In fact, as the star becomes fully convective, the interface between the radiative core and the convective envelope disappears, together with the high radial gradient of rotation which should be responsible for the amplification of magnetic field. The detection by *EXOSAT* of an X-ray flare in the late M star Gliese 644 C (Tagliaferri, Doyle, & Giommi 1990), though, suggests that magnetic fields are still present in the coronae of late-type M stars, and hints to the existence of some other mechanism of magnetic amplification, such as the distributed dynamo, that has to be invoked to explain the presence of magnetic fields in the coronae of these stars.

In this respect recently Fleming et al. (1993) have investigated the nature of the magnetic dynamo and coronal heating mechanism for a sample of M stars seen in the *ROSAT* all-sky survey. They have considered the dependence of coronal heating efficiency (as measured by L_X/L_{bol} ratios) on M_v for a sample including early M stars previously detected in the Extended Medium Sensitivity Survey (Gioia et al. 1989; Stocke et al. 1991) and optically selected very late M stars, and have found, at odds with our findings, that the heating efficiency remains constant beyond spectral type M5. Although their sample of late M stars is quite similar to ours, their conclusion is based *only* on the lack of significant linear correlation between L_X/L_{bol} and M_v, in the entire range of M stars. In our opinion, this is not a conclusive argument since there is expectation of rapid (i.e., nonlinear) change of effectiveness of stellar dynamos due to changes of stellar structure (Mullan 1984). We feel that the kind of analysis we have presented in the previous section is, in this respect, more conclusive because we have made no assumptions on the slope of decline of dynamo efficiency and because our analysis is based on an "unbiased" sample. We note, however, that the statistical size both of this work and of the Fleming et al. sample of late M stars is small and results are very sensitive to inclusion of few data points. Unfortunately, since the X-ray luminosity functions of the M stars seen with *ROSAT* are not yet available, we cannot apply our analysis to the sample of late M stars presented by Fleming and collaborators.

5.2. *X-Ray Emission and Age*

The observed correlation between decreasing X-ray emission and increasing stellar age is generally interpreted as a consequence of the angular momentum loss via magnetic braking (Schatzman 1962; Weber & Davis 1967). We have confirmed, with our sample of stars, that this correlation is present at high significance level (bove 3 σ) for the disk K and early M stars, while for the late M stars the statistical significance of this correlation is lower (slightly above 1 σ). This weak result is likely due to the small sizes of the two samples we are comparing, or can be interpreted as an indication that spin-down is ineffective in these stars, and/or rotation (with the associated "classical" stellar dynamo) is not an important physical mechanism to explain the observed X-ray emission. Unfortunately present instruments make direct measurements of rotation of late and very faint stars very difficult, so we lack any direct evidence on the influence of rotation on coronal magnetic amplification.

In Figure 13 we report the mean values of the X-ray luminosities of A, F, G, K, early M, and late M stars of the Pleiades (Micela et al. 1990), the Hyades (Micela et al. 1988), and the field stars (A and F stars from Schmitt et al. 1985, G stars from Maggio et al. 1987, K, early M, and late M stars from the present work). We may notice that the decrease of X-ray luminosity as a function of increasing age (from top to bottom) is faster for the early M stars than for the K stars suggesting a dependence of this correlation on spectral type.

Further studies are required to better assess this point, with better data including more reliable age indicators for the field stars, and a more reliable determination of the mean value of the X-ray luminosity for the Pleiades M stars, since the presently available value had to be considered, in a strict sense, as an upper limit due to the sensitivity threshold of the *Einstein* IPC observations.

In Figure 12 we have shown that the X-ray luminosity may be used as an age indicator at the same level as the kinematical properties. We note that this method of estimating the ages of stars, if properly calibrated, could provide a better view of the structure and evolution of the stellar population in the Galaxy, especially considering the new data taken with the full-sky survey of *ROSAT* and the future more sensitive observations that will be possible with the XMM and AXAF missions.

5.3. *Dependence of L_X on L_{bol}*

Pallavicini, Tajliaferri, & Stella (1990), studying a sample of flare M stars observed by *EXOSAT*, found a very good corre-

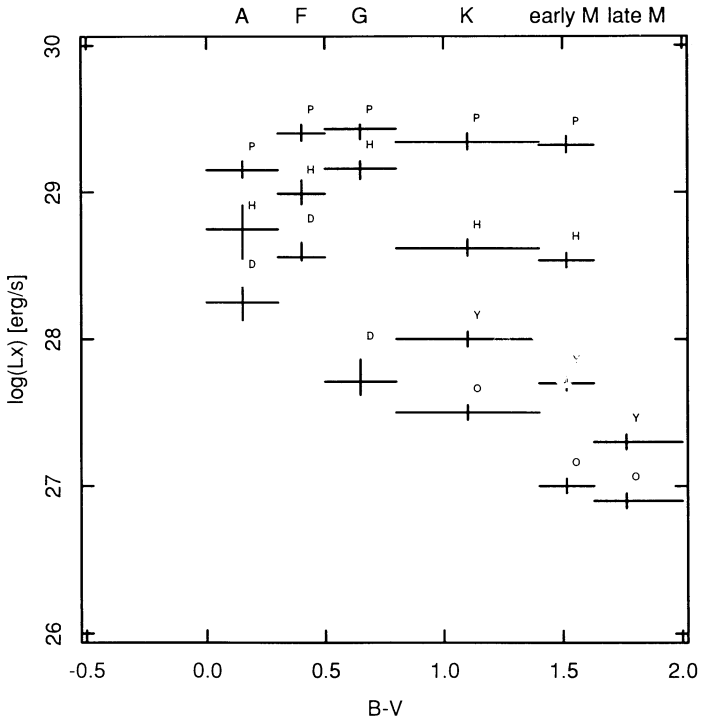

FIG. 13.—The mean values of log (L_X) for the A, F, G, K, early M, and late M stars are reported for the Pleiades [P] (Micela et al. 1990), the Hyades [H] (Micela et al. 1988), and the field stars [D] (A and F from Schmitt et al. 1985, G from Maggio et al. 1987), and K, early M, and late M from the present work ([YD] for young disk and [OD] for old disk stars, respectively).

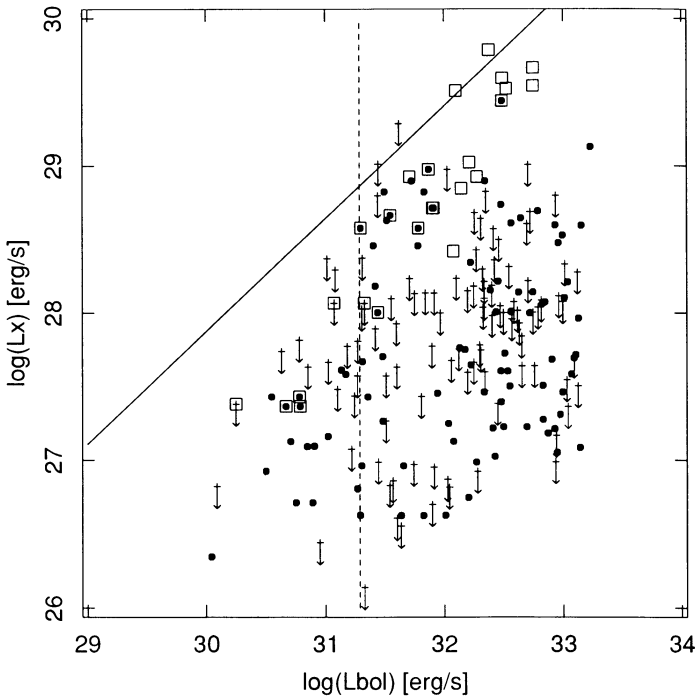

FIG. 14.—L_X vs. L_{bol} for the representative sample of K and M stars. *Solid dots*: detection; *arrows*: upper limits; vertical dashed line corresponds to $M_v = 13.4$; and solid oblique line corresponds to constant X-ray surface flux with log (F_X) = 7.3 ergs s^{-1} cm^{-2}, a value typical of active solar regions. *Squares*: flare stars from our X-ray sample observed with *EXOSAT* (Pallavicini et al. 1990).

lation between X-ray and bolometric luminosities. In Figure 14 we have plotted log (L_X) versus log (L_{bol}) for the representative subsample of K and M stars. The squares indicate the flare stars of Pallavicini et al. (1990) included in our sample. We notice that the good correlation found by Pallavicini et al. (1990) in the case of flare stars cannot be extended to the entire sample of M stars; indeed flaring stars seem to mark a saturation in the X-ray luminosity level. The vertical dashed line separates late M (on the left) from early M stars, while the oblique solid line marks log (L_X) versus log (L_{bol}) for a constant X-ray surface flux equal to log (F_X) = 7.3 ergs s^{-1} cm^{-2}, a typical value of active solar regions assumed to cover the entire stellar surface. We note that this saturation limit seems to reproduce well the observed saturation for K and early M stars, while for late M stars the "actual" saturation marked by detections is about a factor 5 lower. This fact can be interpreted in two simple ways: the active regions of late M stars have a lower X-ray flux [log (F_X) ~ 6.6 ergs s^{-1} cm^{-2}] or the maximum filling factor for late M stars is about one-fifth of that of the K and early M stars. In any case, the coronal activity level of late M stars is significantly lower than that observed in K and early M stars.

5.4. *Contribution to the Soft X-Ray Background*

The estimate of the stellar contribution to the soft X-ray background requires the knowledge of the X-ray luminosities of star populations, the assumption of a model of stellar galactic distribution and of the absorbing interstellar medium, and the assumption of an X-ray emission spectrum of the stars. Since the paper of Rosner et al. (1981), several authors have evaluated the contribution of stellar coronal sources to the diffuse soft X-ray background (Kahn & Caillault 1986; Caillault et al. 1986; Caillault 1990).

More recently, using the spatial distribution of stars taken from the Bahcall & Soneira galaxy model (1980), a continuous emission measure distribution of coronal temperatures, and a mean value of log (L_X) = 28.2 ergs s^{-1} for the M stars, Schmitt & Snowden (1990) estimated a negligible contribution to the background in the C energy band (0.16–0.28 keV), but a contribution up to 40% in the Galactic plane, and less than 10% at higher Galactic latitudes in the M1 and M2 energy bands (~0.4–1.1 keV), and I and J energy bands (~0.8–2.2 keV).

Kashyap et al. (1992) have performed a detailed calculation taking into account the spatial distribution of stars as described by the Bahcall & Soneira galaxy model, a detailed hydrogen distribution along the line of sight, both two temperature and continuous emission measure models for stellar coronal spectra, and the full set of stellar X-ray luminosity functions available at the end of 1990. These authors estimate that, at high latitudes, the stellar contribution to the diffuse soft X-ray background is less than 3% below 0.3 keV, 3%–17% in the medium energy M1 and M2 bands, and 10%–30% in the higher energy bands I and J. At low latitudes they estimate a contribution less than 3% below 0.3 keV, 7%–40% in the medium energy bands, and 27%–70% in the I and J bands.

Using an approach which takes care of the age dependence of X-ray luminosity, plasma temperature, and galactic distribution of stars for ages ranging between ~$10^{7.5}$ and 10^{10}, Micela (1991) has estimated a stellar contribution to the X-ray back-

ground in the energy range 0.16–3.5 keV of about 50% of the X-ray background measured with the IPC (Micela et al. 1991) in the disk plane, rapidly decreasing to less than 10% at 10° Galactic latitude. The main difference of these last results with respect to those quoted previously is the steep increase of stellar contribution at low Galactic latitudes. This effect is essentially due to the faster increase of the number of young stars of Pleiades age (the brightest ones) in the Galactic plane, with respect to the previously adopted Galaxy models.

The X-ray luminosity functions we have found in the present work for K, early M, and late M stars, separately for the young disk and old disk populations (age $\sim 10^{8.5}$ and $\sim 10^{10}$ yr), could allow a further refinement of all these estimates. From a preliminary comparison of our X-ray luminosity functions of M stars with those adopted by Rosner et al. (1981), Caillault et al. (1986), Schmitt & Snowden (1990), and Kashyap et al. (1992), we expect that the contribution of the Galactic disk stars to the soft X-ray background should be slightly lower than previously computed. A detailed calculation will be presented elsewhere.

6. SUMMARY

We have built a sample of 1681 stars of spectral types K or M and luminosity classes IV, V, or VI, within 25 pc from the Sun, by a critical merging of three optical catalogs, and have obtained a sample ~30% wider than the one in the *Catalogue of Stars within 25 Parsecs of the Sun* (Woolley et al. 1970) only. We have investigated the spatial completeness of this optical sample as a function of absolute visual magnitude, showing that the subsample of K stars may be considered spatially complete within 25 pc, the subsample of M stars earlier than $M_v \sim 13$ is incomplete by a factor 2–3 in the same volume, and that of later M stars is 10 times less numerous than expected in the same volume. We have homogeneously recomputed the U, V, W velocity components of all the stars in the sample and have subdivided them into young disk, old disk, and halo population stars according to a statistical method based on space velocity components.

From this optical parent sample we have extracted an X-ray sample of 257 stars surveyed with the *Einstein* IPC. For all these stars we have computed the X-ray luminosity, exploiting the final processing of the *Einstein* IPC data (REV-1, Harnden et al. 1984). The analysis of the data of this X-ray star sample has allowed us to identify an X-ray subsample composed by all the K stars within 12 pc from the Sun, all the M stars within 8 pc from the Sun, and only the serendipitous stars at greater distances, as the best available representative sample of the X-ray properties of the optical parent population. Using the X-ray representative subsample we have derived the following main results:

1. We have confirmed on a statistical basis the steep drop in X-ray luminosity for the M stars at about $M_v = 13.4$, suggesting that the early M stars ($M_v \leq 13.4$) and the late M stars ($M_v \geq 13.4$) be considered as separate classes.
2. We have built maximum likelihood cumulative luminosity functions for the K, early M, and late M stars that are the least biased that can be built with available X-ray data, until results from the *ROSAT* full-sky survey will improve the status of our knowledge.
3. Based on kinematical criteria, we have separated old disk and young disk stars, and have confirmed, with high significance level ($>3\ \sigma$), the decrease in X-ray luminosity with age for K and early M stars, and with lower statistical significance ($\sim 1\ \sigma$) for late M stars.
4. We have shown that the X-ray luminosity may be an efficient parameter to subdivide, on a statistical basis, a large sample of late-type stars into young disk and old disk populations.
5. No obvious correlation between X-ray and bolometric luminosities is observed for the representative subsample of K and M stars, while it is present for the flare stars which also seem to mark a saturation in X-ray luminosity level. For late M stars the saturation marked by detections is about a factor 5 lower with respect to the early M and K stars.

This work was inspired by the late G. S. Vaiana, who took part in its early development and without whose contributions this paper might never have been. We thank the referee J. P. Caillault for his constructive suggestions and comments that have certainly improved the quality of our presentation. We acknowledge partial support by Agenzia Spaziale Italiana (ASI) and Ministero della Università e della Ricerca Scientifica e Tecnologica (M. B., S. S., G. M.), IAIF-CNR (M. B.), NASA grants (R. R.), NASA contract NAS-8-30751 (F. R. H.).

REFERENCES

Avni, Y., & Bahcall, J. N. 1980, ApJ, 235, 694
Bahcall, J. N., & Soneira, R. M. 1980, ApJS, 44, 73
Bookbinder, J. A. 1985, Ph.D. thesis, Harvard Univ.
Caillault, J. P. 1990, PASP, 102, 989
Caillault, J. P., & Helfand, D. J. 1985, ApJ, 289, 279
Caillault, J. P., Helfand, D. J., Nousek, J. A., & Takalo, L. O. 1986, ApJ, 304, 318
Chlebowski, T., Harnden, F. R., & Sciortino, S. 1989, ApJ, 341, 427
Damiani, F., & Micela, G. 1993, in preparation
Eggen, O. J. 1973a, PASP, 85, 289
———. 1973b, PASP, 85, 379
———. 1973c, PASP, 85, 542
Favata, F., Micela, G., Sciortino, S. 1992, A&A, 256, 86
Feigelson, E. D., & Kriss, J. A. 1989, ApJ, 338, 262
Feigelson, E. D., & Nelson, P. I. 1985, ApJ, 293, 192
Fleming, T. A., Gioia, I. M., & Maccacaro, T. 1989, ApJ, 340, 1011
Fleming, T. A., Giampapa, M. S., Schmitt, J. H. M. M., & Bookbinder, J. A. 1993, ApJ, 410, 387
Giacconi, R., et al. 1979, ApJ, 230, 540
Gioia, I. M., Maccacaro, T., Schild, R. E., Wolter, A., Stocke, J. T., Morris, L. S., & Henry, J. P. 1989, ApJS, 72, 567
Gliese, W. 1969, Veroff. Astron. Rechen-Inst., Heidelberg, No. 22
Gliese, W., & Jahreiss, H. 1979, A&AS, 38, 423
Golub, L. 1983, in Activity in Red-Dwarf Stars, ed. P. B. Byrne & Rodonò (Dordrecht: Reidel), 83
Gorenstein, P., Harnden, F. R. Jr., & Fabricant, D. G. 1981, IEEE Trans. Nucl. Sci., NS-28, 869
Grillo, F., Sciortino, S., Micela, G., Vaiana, G. S., & Harnden, F. R. Jr. 1992, ApJS, 81, 795
Harnden, F. R. Jr., Fabricant, D. G., Harris, D. E., & Schwarz, J. 1984, SAO. Spec. Rep., No. 393
Harris, D. E., et al. 1990, The *Einstein* Observatory Catalog of IPC X-Ray Sources, in press
Johnson, D. R. H., & Soderblom, D. R. 1987, AJ, 93, 4
Kahn, S. M., & Caillault, J. P. 1986, ApJ, 305, 526
Kashyap, B., Rosner, R., Micela, G., Sciortino, S., Vaiana, G. S., & Harnden, F. R. Jr. 1992, ApJ, 391, 667
Maggio, A., Sciortino, S., Vaiana, G. S., Majer, P., Bookbinder, J., Golub, L., Harden, F. R. Jr., & Rosner, R. 1987, ApJ, 315, 687
Maggio, A., Vaiana, G. S., Haisch, B. M., Stern, R. A., Bookbinder, J., Harden, F. R., Jr., & Rosner, R. 1990, ApJ, 348, 253
Mangenay, A., & Praderie, F. 1984, A&A, 130, 143
Marcy, G. W., & Chen, G. H. 1992, ApJ, 390, 550
Marilli, E., & Catalano, S. 1984, A&A, 133, 57
Meusinger, H., Reimann, H. G., & Stecklum, B. 1991, A&A, 245, 57
Micela, G. 1991, Ph.D. thesis, Univ. Palermo
Micela, G., Sciortino, S., & Serio, S. 1984, in X-ray Astronomy '84, ed. M. Oda & R. Giacconi (Tokyo: Inst. of Space and Astronautical Science), 43
Micela, G., Sciortino, S., Vaiana, G. S., Schmitt, J. H. M. M., Stern, R. A., Harnden, F. R. Jr., & Rosner, R. 1988, ApJ, 325, 798

Micela, G., Sciortino, S., Serio, S., Vaiana, G. S., Bookbinder, J., Golub, L., Harnden, F. R. Jr., & Rosner, R. 1985, ApJ, 292, 172
Micela, G., Harnden, F. R. Jr., Rosner, R., Sciortino, S., & Vaiana, G. S. 1991, ApJ, 380, 495
Micela, G., Sciortino, S., Vaiana, G. S., Harnden, F. R. Jr., Rosner, R., & Schmitt, J. H. M. M. 1990, ApJ, 348, 557
Mullan, D. J. 1984, ApJ, 282, 603
Pallavicini, R., Golub, L., Rosner, R., Vaiana, G. S., Ayres, T., & Linsky, J. L. 1981, ApJ, 248, 279
Pallavicini, R., Tagliaferri, G., & Stella, L. 1990, A&A, 282, 403
Parker, E. N. 1979, *Cosmical Magnetic Fields* (Oxford: Clarendon)
Pettersen, B. R. 1982, in IAU Colloq. 102, Activity in Red-Dwarf Stars, ed. Patrick B. Byrne & Marcello Rodonó (Dordrecht: Reidel), 17
Rosner, R., et al. 1981, ApJ, 249, L5
Rosner, R., Golub, L., & Vaiana, G. S. 1985, ARA&A, 23, 413
Schatzman, E. 1962, Ann. d'Astrophys., 25, 18
Schmitt, J. H. M. M. 1985, ApJ, 293, 178
Schmitt, J. H. M. M., Collura, A., Sciortino, S., Vaiana, G. S., Harnden, F. R. Jr., & Rosner, R. 1990b, ApJ, 365, 704
Schmitt, J. H. M. M., Golub, L., Harnden, F. R. Jr., Maxson, C. W., Rosner, R., & Vaiana, G. S. 1985, ApJ, 290, 307
Schmitt, J. H. M. M., Micela, G., Sciortino, S., Vaiana, G. S., Harnden, F. R. Jr., & Rosner, R. 1990a, ApJ, 351, 492
Schmitt, J. H. M. M., & Snowden, S. L. 1990, ApJ, 361, 207
Schmidt, M. 1968, ApJ, 151, 393
Sciortino, S., Harnden, F. R. Jr., Rosner, R., Schmitt, J. H. M. M., & Vaiana, G. S. 1990, ApJ, 361, 621
Sciortino, S., & Micela, G. 1992, ApJ, 595, 388
Stauffer, J. R., & Hartmann, L. W. 1986, PASP, 98, 1233
Stern, R. A., Zolcinski, M. C., Antiochos, S. K., & Underwood, J. H. 1981, ApJ, 249, 647
Stocke, J. T., et al. 1991, ApJS, 76, 813
Tagliaferri, G., Doyle, J. G., & Giommi, P. 1990, A&A, 231, 131
Upgren, A. R. 1978, ApJ, 83, 626
Upgren, A. R., & Armandroff, T. E. 1981, ApJ, 86, 1898
Vaiana, G. S., et al. 1981, ApJ, 245, 163
Walter, F. M., Linsky, J. L., Simon, T., Golub, L., & Vaiana, G. S. 1984, ApJ, 281, 815
Weber, E. J., Davis, L. 1967, ApJ, 148, 217
Wielen, R., Jahreiss, H., & Kruger, R. 1983, in IAU Colloq. 76, The Nearby Stars and the Luminosity Function, ed. A. G. Davis Phillips & A. R. L. Upgren (Schenectady: Davis), 163 (WJK)
Wooley, R. E. E. A., Penstom, M. J., & Pocock, S. B. 1970, R. Obs. Ann. 5, 281, 815